# Robust Indirect Vector Control of Induction Motor Fed by Voltage Source Inverter for Multi-Source Electric Vehicle

By

**Bushra Hafeez**

**Fall-2021-MS-EE 00000363450 SEECS**

Supervisor

**Dr. Kamran Zeb**

A thesis submitted in partial fulfillment of the requirements for the degree of Masters of science in Electrical in Engineering (MS EE)

In

School of Electrical Engineering & Computer Science (SEECS) ,

National University of Sciences and Technology (NUST),

Islamabad, Pakistan.

(December 2023)

## THESIS ACCEPTANCE CERTIFICATE

Certified that final copy of MS/MPhil thesis entitled "Robust Indirect Vector Control of Induction Motor Fed by Voltage Source Inverter for Multisource Electric Vehicle" written by Bushra Hafeez, (Registration No 363450), of SEECS has been vetted by the undersigned found complete in all respects as per NUST Statutes/Regulations, is free of plagiarism, errors and mistakes and is accepted as partial fulfillment for award of MS/M Phil degree. It is further certified that necessary amendments as pointed out by GEC members of the scholar have also been incorporated in the said thesis.

Signature: _____

Name of Advisor: _____Dr. Kamran Zeb_____ __

Date: _____04-Dec-2023_____ __

HoD/Associate Dean:_____

Date: _____

Signature (Dean/Principal): _____ ___

Date: _____ __

# Approval

It is certified that the contents and form of the thesis entitled "Robust Indirect Vector Control of Induction Motor Fed by Voltage Source Inverter for Multisource Electric Vehicle" submitted by Bushra Hafeez have been found satisfactory for the requirement of the degree

Advisor :   Dr. Kamran Zeb

Signature: _____

Date: _____04-Dec-2023_____

Committee Member 1:Dr. Waqar Uddin

Signature: _____

05-Dec-2023

Committee Member 2:Dr. Jawad Arif

Signature: _____

Date: _____04-Dec-2023_____

Signature: _____

Date: _____

ii

# Dedication

**DEDICATED TO**
**MY**
**"ADORABLE PARENTS"**

Who taught me!

The first word to speak

The first alphabet to write

AND

The first step to take

Who always wished to see me successful in every field of life

Who are like a shady tree for me in the scorching sun of life

Whose love will never mitigate

AND

Whose prayers will never die

Who are nearest, dearest and deepest to me

May ALLAH give them a long, happy and healthy life

(Ameen)

# Certificate of Originality

I hereby declare that this submission titled "Robust Indirect Vector Control of Induction Motor Fed by Voltage Source Inverter for Multisource Electric Vehicle" is my own work. To the best of my knowledge it contains no materials previously published or written by another person, nor material which to a substantial extent has been accepted for the award of any degree or diploma at NUST SEECS or at any other educational institute, except where due acknowledgement has been made in the thesis. Any contribution made to the research by others, with whom I have worked at NUST SEECS or elsewhere, is explicitly acknowledged in the thesis. I also declare that the intellectual content of this thesis is the product of my own work, except for the assistance from others in the project's design and conception or in style, presentation and linguistics, which has been acknowledged. I also verified the originality of contents through plagiarism software.

Student Name:Bushra Hafeez

Student Signature: _____

# Acknowledgments

All praises and thanks are for ALMIGHTY ALLAH the compassionate, the merciful, the only creator of the universe and the source of all knowledge and wisdom who blessed me with health, thoughts, talented teachers, cooperative friends and opportunity to make some contribution to the already existing ocean of knowledge. I offer my humblest thanks to the greatest social reformer HOLY PROPHET MUHAMMAD (PBUH) who is the most perfect and forever a great model of guidance for humanity.

I avail this opportunity in recording my sincerest and deepest thanks to my honorable supervisor, Dr. Kamran Zeb, Assistant Professor, School of Electrical Engineering and Computer Science,National University of Sciences and Technology (NUST),Islamabad. I owe a great debt of gratitude to him for his affectionate help, valuable suggestions, invaluable guidance and sympathetic attitude during my studies and presentation of this manuscript.

I would also like to acknowledge with a deep sense of gratitude to my committee members Dr. Waqar Uddin, Assistant Professor, National University of Technology, Islamabad. and Dr. Jawad Arif, Assistant Professor, School of Electrical Engineering and Computer Science,National University of Sciences and Technology (NUST),Islamabad for their wise counsel and dexterous guidance.

Last but not the least I pay my cordial thanks to those whose love will never mitigate and whose prayer will never die, My Loving Mother and My Dear Father, Muhammad Hafeez whose hands always raised in prayer for me and whose inspirations have ever been a tower of light for me. Words are lacking to express my humble obligations to my sisters for their encouragement and affections in providing me an atmosphere conductive to the perusal of academic goals.

**Bushra Hafeez**

# Abstract

Hybrid electric vehicles are gaining popularity due to exponential decrease in oil and natural gas resources. In order to prevent the terrible consequences of greenhouse gas emissions and global warming, it is crucial to utilize renewable energy sources.The field of clean energy generation and efficient utilization is experiencing significant growth in research. The hybrid energy storage system (HESS) of the proposed hybrid electric vehicle consists of fuel cell (FC), battery, supercapacitor (SC)and a photovoltaic(PV), which are connected to the DC bus through the DC-DC power converters. The DC bus is subsequently linked to an inverter,Space Vector Pulse Width Modulation (SVPWM) technique has been used for three phase Voltage Source Inverter to control electric motor of the vehicle. In rough driving circumstances the behaviour of components such as energy sources, induction motors, and power processing blocks significantly deviates from their typical behavior due to non linear nature of vehicle model. Barrier function based adaptive sliding mode controller has been used to ensure the finite- time convergence of the output variable even when the upper bound of the disturbances is unknown. The performance of the proposed barrier function-based adaptive sliding mode controller technique is analyzed via simulations on MATLAB/Simulink,. The proposed strategy has been validated through real time hardware-in-the-loop (HIL) experiments using C2000 Delfino Microcontroller F28379D Launchpad.

# Contents

# List of Tables

# List of Figures

# List of Abbreviations and Symbols

## Abbreviations

**EV**          Electric Vehicle

**PV**          Photovoltaic

**SC**          Supercapacitor

**FC**          Fuel Cell

**HESS**          Hybrid Energy Storage System

**IVC**          Indirect Vector control

**SMC**          Sliding Mode Controller

**BFASMC**          Barrier Function based Adaptive Sliding Mode Controller

**HIL**          Hard-ware in Loop

**IM**          Induction Motor

**IFOC**          Indirect Field Oriented Control

**IM**          Induction Motor

**PWM**          Pulse Width Modulation

**IM**          Induction Motor

# Introduction and Motivation

The accelerating depletion of conventional energy resources, particularly fossil fuels, is a major contributor to the world's ongoing environmental challenges. The large increase in gasoline use hastens the breakdown of the ozone layer, resulting in a variety of negative climatic impacts. As a result of these issues, the international community has decided to shift towards environmentally sustainable energy sources.[15]This advancement has piqued the curiosity of researchers in power transmission and hybrid energy storage systems.The transport industry has made significant contributions to world progress. Conventional automobiles that are powered by internal combustion engines (ICEs) are dependent on fossil fuels, which results in problems such as pollutants and the expense of petroleum.Dr. Ferdinand Porsche introduced the first hybrid electric vehicle in 1898 in to address these concerns.[9]

Electric vehicles (EVs) are a potential alternative to conventional automobiles that aim to conserve energy and reduce petroleum usage. EVs are also environment friendly, with no emissions, and produce less noise. Researchers are currently facing the issues of lowering costs while improving the durability and general performance of electric vehicles. Energy-efficient vehicles (EVs) require high-power and energy-density energy storage devices (ESDs) to improve efficiency and range. Storage devices with a high power density have the capacity to charge and discharge quickly.[10] The advantage of high energy density electric vehicles (EVs) is their ability to drive long distances. Supercapacitors (SCs) have a high power density and a long lifespan, but they also have higher energy expenditures and a lower energy density. Batteries, on the other hand, have a high energy density, but at the expense of a shorter lifespan and lower power density.

Presently, the vehicular environment is extraordinarily dynamic. It is necessary for a vehicle to perform frequent start-stop, rapid acceleration, and uphill-downhill manoeuvres. Automobiles

are subjected to frequent instances of starting and stoping, in addition to sudden surges in velocity. The subsequent torque and speed requirements of the vehicle demonstrate a significant level of unpredictability. The lack of steady-state operation among the vehicle's components is brought about by the acceleration and deceleration of auxiliary loads, which result in abrupt changes in load torque. Nonlinearities are anticipated to exert a substantial influence on the operation of hybrid electric vehicle (HEV) components, such as traction motors, power converters, and energy sources, due to the dynamic operating conditions.

Since its inception, the AC asynchronous motor, also known as the induction motor, has become the most widely used electrical motor and has amassed considerable notoriety. An important advantage of induction motors is their capability to function independently of any connections between the stationary and rotating components.[3] The indirect vector control of an induction motor depends on the self-inductance of the rotor $L_r$, rotor resistance $R_r$, and mutual inductance $L_m$.The resistance of the rotor is significantly influenced by the machine's temperature, whereas the inductances vary in response to both temperature and machine saturation.Rotor flux and torque performance will deteriorate due to any discrepancy between the parameters; this degradation will manifest as steady-state error and transient performance degradation. Therefore, it is crucial to consistently modify the controller parameters. The resultant HEV system is therefore a complex nonlinear system, which makes the design of the controller a difficult task..

## 1.1 Problem Statement and Contribution

The mathematical models of hybrid electric vehicles (HEVs) exhibit significant dynamical and nonlinear characteristics. Consequently, the utilization of nonlinear controllers may offer superior performance compared to their linear equivalents. This is due to the ability of nonlinear controllers to effectively address the inherent non-linearities and parametric variations/uncertainties present within the system.

The non-linear nature of induction motors renders linear controllers, such as the PI controller, ineffective in achieving optimal performance. Nevertheless, fixed gain controllers exhibit a high degree of sensitivity to variations in parameters, load disturbances, and other external factors. To solve these problems, intelligent controller such as sliding mode controller (SMC) and BFASMC are proposed for sensor-less vector control. SMC is a robust control because the feedback input with high gain cancels the nonlinearities, parameter uncertainties and external disturbances. However, one of the drawbacks of this controller is the chattering phenomenon

that arises due to the discontinuous nature of the control action. The BFASMC is proposed as a solution to address the issue of chattering and enhance the process of gain selection.The advantages of adaptive barrier function based sliding mode controller are as follows:

- To implement the robust indirect vector control of induction motor.

- To devise a system model that does not involve integral terms in order to reduce computational complexities.

- Gain of the adaptive barrier function based sliding mode controller is not overestimated which helps in minimizing chattering effect.

- Its performance is robust and efficient with zero steady-state error.

- Finite-time convergence to a predefined neighborhood of zero irrespective of knowledge of upper bound of disturbance.

This study is intended to demonstrate the following points:

- Mathematical modeling of HESS and induction motor

- HESS comprises of four energy sources: fuel cell, battery, supercapacitor, and PV panel to meet energy demands.

- Indirect field oriented control of induction motor.

- Comparison of SMC and adaptive barrier function based sliding mode controller is performed using simulation and as well as experimental for DC bus voltage and speed tracking of induction motor for load disturbances.

# Literature Review

Various energy management strategies for HESS of HEVs are suggested in the literature. A multiobjective optimisation approach for the energy management of hybrid electric vehicles, utilising the Radau pseudospectral method, was suggested in reference [4]. It offers a dependable and rapid method for optimising multiple objectives in order to manage the energy of HESS in electric vehicles. A Markov driving pattern recognizer-based multi-mode predictive energy management system for fuel cell hybrid electric vehicles was developed in [13]. This method has increased the fuel cell system's durability and decreased its fuel consumption. An energy optimisation strategy for HESS of EVs with two or more ESDs was proposed in [17] . It enhances energy source performance, fuel economy, and longevity, all of which are critical for the energy management system of electric vehicles. Adaptive EMS based on model predictive control has been suggested for plug-in hybrid electric vehicles in [22], but velocity prediction only employs a deep neural network. A model of driver behaviour must be developed for intelligent EMS in PHEVs.

The implementation of rule-intersecting deep reinforcement learning-based EMS for HEVs was discussed in [7]. It improves fuel economy and stabilises the energy management system, but requires a substantial quantity of memory for optimal operation. A multi-neural network-based predictive EMS for multi-mode plug-in HEVs was proposed in [11], but battery degradation, which could increase the economic potential of PHEVs, was not accounted for. A study [5] developed a reinforcement learning-based stochastic model predictive control system for energy management in plug-in HEVs. This system improved fuel economy but requires further development in terms of performance. An energy management system for HEVs based on a real-time bi-adaptive controller was proposed in [19]. The system reduced power losses, temperature, and battery fatigue, but it was not physically implemented.

Dynamic programming and optimal EMS based on a receding horizon for HEVs has been implemented in [14], but it required redundant memory and recursive function calls. [12] proposes a control-based perturbation observer that is robust for the HESS of EVs. A proposal for a HESS of EVs using fuzzy logic-based EMS was made in [21], but it is contingent on human knowledge and its rules must be routinely updated. A battery and superconducting magnetic hybrid energy storage system for energy management, as well as an intelligent EMS based on driving pattern recognition, have been implemented in reference [6]. In [18] a HESS of EV utilising pulse width modulation was developed. Although pulse width modulation is an effective technique, it is complicated and costly. An HESS for EVs based on machine learning methods was developed in [16], which reduced the operational cost of an electric vehicle. However, the performance of the proposed EMS has not been validated in that study. A sliding mode control-based HESS for HEVs was proposed in [9]. Peak values and steady-state error in DC bus voltage are, however, substantial when the load changes. Additionally, integral elements result in a slower system. The HESS of electric vehicles was developed utilising adaptive terminal sliding mode control in [20] . However, the study does not take into account the specific characteristics of the vehicles. Field orientation was a concept introduced by F. Blaschke in 1972 with the intention of imbuing an induction motor with attributes akin to those of a DC motor. He utilised a decoupled control strategy, which he termed trans-vector control, to regulate the torque and flux within the motor. The stator current components along the d and q axes are autonomously regulated in a vector control scheme. The q component regulates the torque, while the d component governs the flux linkage. On the basis of the rotor flux angle acquisition, the VC strategy is divided into two groups: Direct Vector Control (DVC) and Indirect Vector Control (IVC).The DVC strategy directly measured the flux angle of the rotor, whereas the IVC scheme estimates the angle.

In high-performance applications, indirect field-oriented techniques are now widely used to control induction motor drives. [8]The decoupling of torque and flux control of the induction motor is ensured using field-oriented techniques; furthermore, the induction motor can be linearly controlled as if it were a separately excited D.C. motor. Nevertheless, the uncertainties continue to impact the control performance of the resultant linear system. These uncertainties typically consist of unforeseeable fluctuations in parameters, disturbances caused by external loads, unmodeled and nonlinear dynamics, and so forth. Consequently, numerous investigations have been conducted on motor drives to ensure optimal performance amidst fluctuations in parameters and external load disturbances. These investigations have encompassed various control strategies, including adaptive control,nonlinear control, and variable structure system control.

CHAPTER 3

# Methodology

## 3.1 System Model

This section offers a brief summary of the main elements of a Hybrid Electric Vehicle (HEV), which include the hybrid energy storage system, power converters, inverter, and three-phase induction motor. Furthermore, the HESS (Hybrid Energy Storage System) has four separate energy sources: the fuel cell, super-capacitor, PV, and battery.

### 3.1.1 Fuel Cell

The fuel cell (FC) is an environmentally-friendly energy source with exceptional efficiency. The energy is generated through a chemical process involving hydrogen and oxygen in the presence of an electrolyte. The DC-DC boost converter is used to connect the FC voltage to the DC bus, increasing its voltage. This converter utilises a high-frequency inductor $L_1$ with internal resistance $R_1$, a single insulated gate bipolar transistor (IGBT), and a filtering capacitor C. In order to overcome the limits of fuel cells, other sources are utilized in conjunction with them. This integration improves the distance that may be driven and reduces the strain on each separate power source. As a result, the longevity of the sources is also extended.

### 3.1.2 Battery

A rechargeable device, known as the battery, is responsible for storing low-speed energy generated during deceleration mode and regenerative braking.The battery provides a continuous power supply under a steady load. The battery is connected to a DC-DC buck-boost converter
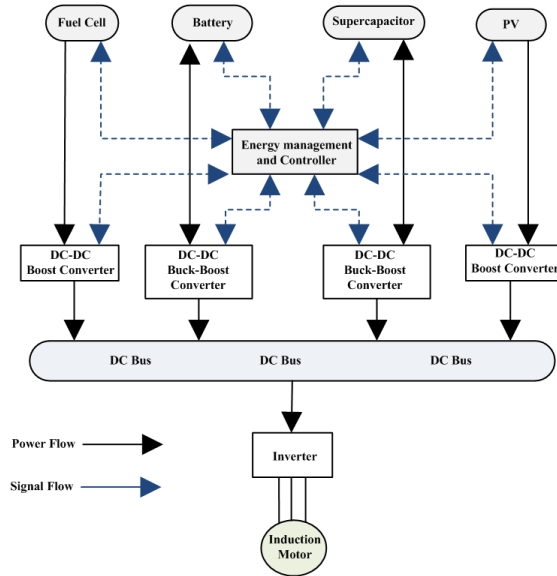
**Figure 3.1:** Block diagram of proposed system

to adjust the battery voltage to meet the voltage level of the DC bus, either by increasing or decreasing it. The converter consists of multiple components, namely resistor $R_2$, inductor $L_2$, two IGBT switches ($S_2$ and $S_3$), and two diodes ($D_2$ and $D_3$).

### 3.1.3 Super-Capacitor

The super-capacitor (SC) is a capacitor with a high capacitance. Super-capacitors are well-suited for integration into hybrid electric vehicles (HEVs) because of their exceptional power density, compact dimensions, rapid charging capability, and capacity to efficiently capture the maximum amount of regenerative energy. Super-capacitors exhibit a significantly extended lifespan compared to batteries, with an estimated 1 million recharge cycles. A bidirectional DC–DC buck-boost converter has been utilised for power regulation. This converter consists of a resistor $R_3$, an inductor $L_3$, two IGBTs with switches $S_4$ and $S_5$, and two diodes $D_4$ and $D_5$.

### 3.1.4 PV

The installation of PV panels is done in the configuration of strings, with each string consisting of 15 panels. Each individual panel has a power output of 65W. The panels are arranged in a way that enables their combined output to reach 1.35 kilowatts.

The energy output of PV panels is directly affected by temperature and solar radiation. Photovoltaic (PV) systems are a renewable and eco-friendly means of generating electricity without

any associated costs. The PV panel is connected to a DC-DC boost converter to raise the PV voltage to match the DC bus voltage. The converter consists of various components, specifically resistor $R_4$, inductor $L_4$, capacitance $C_2$, IGBT switch $S_6$, and diode $D_6$.

### 3.1.5 Inverter

Space Vector Modulation (SVM) was originally developed as a vector-based alternative to Pulse Width Modulation (PWM) for three phase inverters. The inverter output voltage is regulated by utilising the space vector idea, derived from the spinning field of the induction motor. The three phase qualities in this modulation approach are converted into their corresponding two phase quantities in either a fixed frame or a frame that rotates synchronously. The magnitude of the reference vector can be ascertained based on the two-phase components and then employed to modulate the output of the inverter. The space vector PWM (SVPWM) approach is highly efficient for variable frequency drive applications.This technique is quite advanced and requires a significant amount of computer power. It optimises the utilisation of the direct current input voltage and minimises the presence of harmonic distortion in the output voltages or currents that are supplied to the phases of an alternating current motor.

### 3.1.6 Induction Motor

Difficult driving conditions require a motor that can efficiently operate under different load requirements. Choosing the right motor for an electric vehicle is crucial as it has a substantial influence on the vehicle's overall performance. Previous study has shown that electric motors have faster acceleration and greater torque precision than internal combustion engines. Multiple commercially available electric motor types include DC motors, induction motors, brush-less permanent magnet motors, and switching reluctance motors. However, induction motors have demonstrated greater suitability in automobile technology compared to the other available solutions. Hybrid electric vehicles favour these motors above others due to their robustness, cost effectiveness, extended lifespan, easy availability, and wide speed range.

## 3.2 Mathematical Modeling

Analyzing the performance of a hybrid electric vehicle under different operating conditions using a mathematical model is possible.The mathematical model has been derived by applying
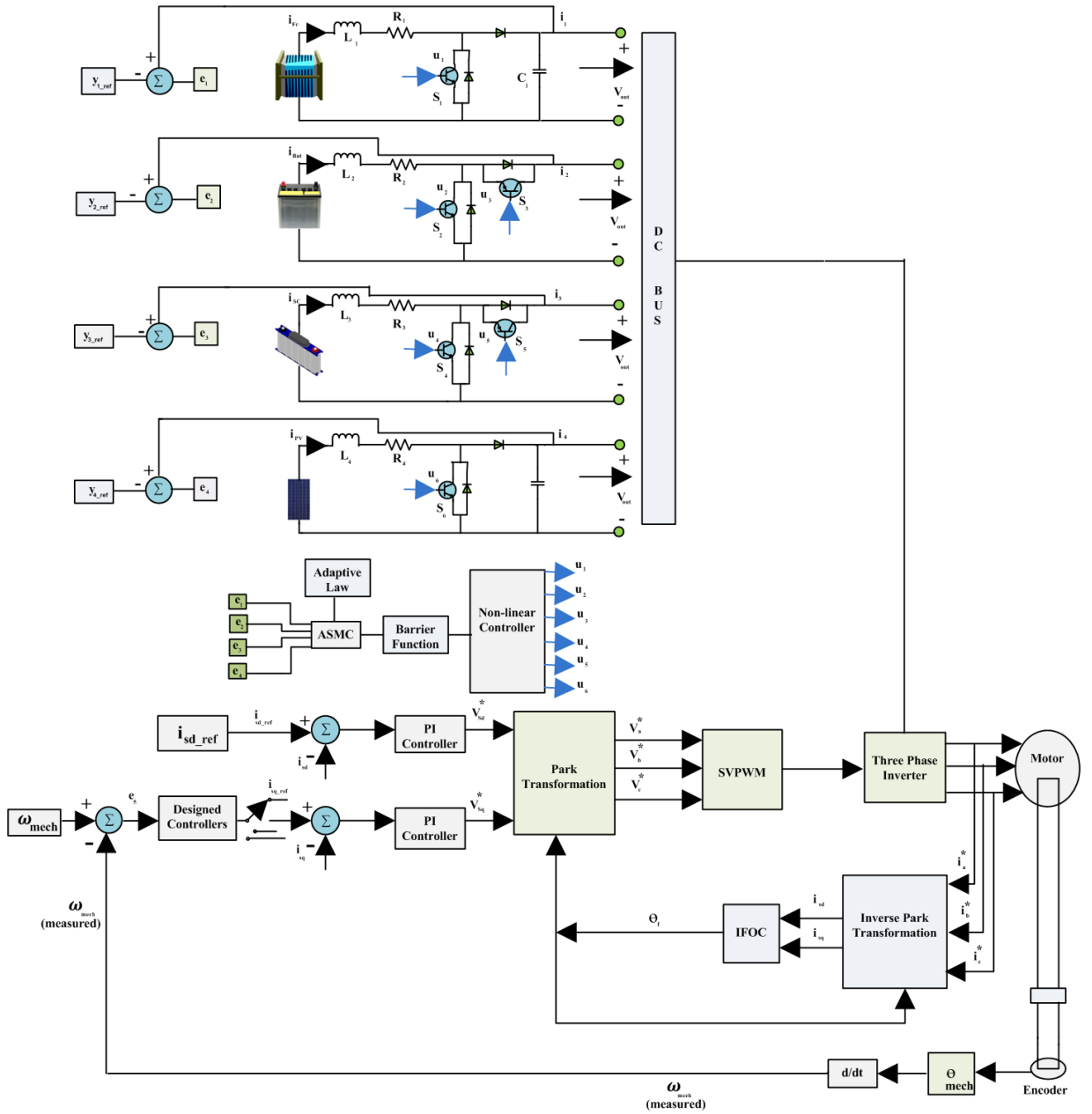
**Figure 3.2:** Proposed Model of IVC

fundamental electrical laws and performing averaging across the whole duty cycle.

### 3.2.1   Mathematical Modeling of HESS

The HESS state-space dynamical model being discussed is defined as follows:

$$\dot{y}_1 = \frac{v_{fc}}{L_1} - \frac{R_1 y_1}{L_1} - \frac{y_5(1-a_1)}{L_1} \tag{3.2.1}$$

$$\dot{y}_2 = \frac{v_{bat}}{L_2} - \frac{R_2 y_2}{L_2} - \frac{y_5 a_{23}}{L_2} \tag{3.2.2}$$

$$\dot{y}_3 = \frac{v_{sc}}{L_3} - \frac{R_3 y_3}{L_3} - \frac{y_5 a_{45}}{L_3} \tag{3.2.3}$$

$$\dot{y}_4 = \frac{v_{pv}}{L_4} - \frac{R_4 y_4}{L_4} - \frac{y_5(1-a_6)}{L_4} \tag{3.2.4}$$

$$\dot{y}_5 = \frac{y_1(1-a_1)}{C} + \frac{y_2 a_{23}}{C} + \frac{y_3 a_{45}}{C} + \frac{y_4(1-a_6)}{C} - \frac{i_0}{C} \tag{3.2.5}$$

The variables $y_1$, $y_2$, $y_3$, $y_4$, and $y_5$ correspond to the FC current, battery current, SC current, PV current, and DC bus voltage, respectively. The parameters R, C, and L correspond to resistance, capacitance, and inductance, respectively. The variables $v_{fc}$, $v_{bat}$, $v_{sc}$, $v_{PV}$, and $i_0$ correspond to the voltage across the fuel cell (FC), the voltage across the battery, the voltage across the supercapacitor, the voltage across the photovoltaic (PV) system, and the current passing through the load, respectively. The system's control inputs are represented by the variables $a_1$, $a_{23}$, $a_{45}$, and $a_6$. The PWM duty cycles are utilised to control the operation of the IGBT switches. The IGBT switches regulate the output of the converter. The switch has two states: one is the ON position and the other is the OFF position. The duty cycle represents the proportion of time during one cycle that the switch is in the on state, expressed as a percentage. The control inputs for achieving the desired output from power converters are determined by the duty cycles of the converters.

Deriving the global model is challenging due to the utilisation of buck-boost converters in batteries and supercapacitors, which consist of two switches. The battery can function in two separate modes: charging mode and discharging mode. The control input $a_{23}$ is defined in the following manner:

$$a_{23} = [S(1-a_2) + (1-S)a_3] \tag{3.2.6}$$

The buck-boost converter operates in boost mode when the value of S is 0, and in buck mode when the value of S is 1. The operational mechanism of a supercapacitor closely resembles that of a battery. The average control input $a_{45}$ is precisely specified as:

$$a_{45} = [S(1-a_4) + (1-S)a_5] \tag{3.2.7}$$

### 3.2.2 Mathematical Modeling of Induction Motor

In order to analyze a three-phase circuit, the three-phase supply and current for induction motor modelling are converted to two-phase in the stationary reference frame d-q axis. The voltages along the stator d-q axis can be expressed in terms of flux linkages [1]:

$$\begin{bmatrix} v_{sd} \\ v_{sq} \end{bmatrix} = R_s \begin{bmatrix} i_{sd} \\ i_{sq} \end{bmatrix} + \frac{d}{dt} \begin{bmatrix} \lambda_{sd} \\ \lambda_{sq} \end{bmatrix} + \omega_d \begin{bmatrix} 0 & -1 \\ 1 & 0 \end{bmatrix} \begin{bmatrix} \lambda_{sd} \\ \lambda_{sq} \end{bmatrix} \qquad (3.2.8)$$

The symbol $\omega_d$ represents the derivative of the rotor field angle $\theta_{da}$ with respect to time.

In the equations (3.2.8) mentioned before, each vector consists of two elements. The first element represents the voltage on the d-axis of the stator, while the second element represents the voltage on the q-axis of the stator.The stator flux components of the d-axis and q-axis are denoted as $\lambda_{sd}$ and $\lambda_{sq}$, respectively, and can be expressed as follows:

$$\lambda_{sd} = L_s i_{sd} + L_m i_{rd} \qquad (3.2.9a)$$

$$\lambda_{sq} = L_s i_{sq} + L_m i_{rq} \qquad (3.2.9b)$$

where $L_s = L_{ls} + L_m$

By replacing the flux linkage values with inductance values in the stator voltage calculations described above, we obtain ,

$$v_{sd} = R_s i_{sd} - \omega_d \lambda_{sq} + L_{ls} \frac{d}{dt} i_{sd} + L_m \frac{d}{dt}(i_{sd} + i_{rd}) \qquad (3.2.10a)$$

$$v_{sq} = R_s i_{sq} + \omega_d \lambda_{sd} + L_{ls} \frac{d}{dt} i_{sq} + L_m \frac{d}{dt}(i_{sq} + i_{rq}) \qquad (3.2.10b)$$

The rotor d-q axis voltages are determined by calculating the associated flux linkages.

$$\begin{bmatrix} v_{rd} \\ v_{rq} \end{bmatrix} = R_r \begin{bmatrix} i_{rd} \\ i_{rq} \end{bmatrix} + \frac{d}{dt} \begin{bmatrix} \lambda_{rd} \\ \lambda_{rq} \end{bmatrix} + \omega_{dA} \begin{bmatrix} 0 & -1 \\ 1 & 0 \end{bmatrix} \begin{bmatrix} \lambda_{rd} \\ \lambda_{rq} \end{bmatrix} \qquad (3.2.11)$$

where $\frac{d}{dt}\theta_{dA}=\omega_{dA}$ and $\omega_{dA}=\omega_{sl}=\omega_e\text{-}\omega_r$

The first component in the pair is similar to the d-axis, while the second component is similar to the q-axis [1].The flux connections of the d-q windings can be described as follows in relation to currents:

$$\lambda_{rd} = L_r i_{rd} + L_m i_{sd} \qquad (3.2.12a)$$

$$\lambda_{rq} = L_r i_{rq} + L_m i_{sq} \qquad (3.2.12b)$$

where $L_r = L_{lr} + L_m$ and $L_r$ is the rotor leakage resistance.

When we substitute the values of flux linkages into the above mentioned rotor voltage equations in terms of inductances, we obtain:

$$v_{rd} = R_r i_{rd} - \omega_{dA} \lambda_{rq} + L_{lr} \frac{d}{dt} i_{rd} + L_m \frac{d}{dt}(i_{sd} + i_{rd}) \qquad (3.2.13a)$$

$$v_{rq} = R_s i_{rq} + \omega_{dA} \lambda_{rd} + L_{lr} \frac{d}{dt} i_{rq} + L_m \frac{d}{dt}(i_{sq} + i_{rq}) \qquad (3.2.13b)$$

where $v_{rd} = 0$ and $v_{rq} = 0$ .

The acceleration of the induction motor (IM) can be found by subtracting the load torque from the electromagnetic torque, which both affect the combined inertia (Jeq) of the motor and the load torque.

$$\frac{d\omega_{\text{mech}}}{dt} = \frac{1}{J_{\text{eq}}}(T_{\text{em}} - T_{\text{l}}) \qquad (3.2.14)$$

Equating $T_{\text{em}} = \frac{pL_m}{2}(i_{sq}i_{rd} - i_{sd}i_{rq})$ in above equation we get:

$$\frac{d\omega_{\text{mech}}}{dt} = \frac{\frac{pL_m(i_{sq}i_{rd} - i_{sd}i_{rq})}{2} - T_l}{J_{eq}} . \qquad (3.2.15)$$

The following equation provides the rotor's mechanical speed in radians per second:

$$\omega_{mech} = \frac{2}{p} w_{\text{m}} \qquad (3.2.16)$$

## 3.3   Indirect Field Oriented Control

Two vector control methods that are similar to one another are IVC and DVC.The method used to calculate the rotor field angle is the main difference between the two.The direct FOC measures the orientation of the air-gap flux using a search coil, a hall-effect sensor, or other techniques.However, because special motor modifications are required to install the flux sensors, using sensors is expensive. Moreover, one cannot sense the rotor flux directly. Calculating the rotor flux from a directly received signal may be imprecise at low speeds due to variations in flux level and temperature, as well as the dominance of the stator resistance voltage drop in the stator voltage equation. The flux angle is obtained by estimating techniques in the indirect method.This method uses machine parameters to estimate the field angle.The sum of the rotor and slip speeds is the flux linkage speed.

$$\theta_e = \int \omega_e dt = \int (\omega_r + \omega_{sl}) dt = (\theta_r + \theta_{sl}) \qquad (3.3.1)$$

The equations governing the rotor circuit are as follows:

$$\frac{d}{dt}\lambda_{rd} + \frac{R_r}{L_r}\lambda_{rd} - \frac{L_m}{L_r}\text{ß}_{sd}R_r - \omega_{sl}\lambda_{rd} = 0 \tag{3.3.2}$$

$$\frac{d}{dt}\lambda_{qr} + \frac{R_r}{L_r}\lambda_{rq} - \frac{L_m}{L_r}\text{ß}_{sq}R_r - \omega_{sl}\lambda_{rq} = 0 \tag{3.3.3}$$

During the vector control procedure, the d-axis is precisely aligned with the rotor flux linkage space vector to ensure that the q-axis is devoid of any rotor flux linkage.

$$\lambda_{rq}(t) = 0 \tag{3.3.4}$$

Replacing $\lambda_{rq}$ in Eq. (12b) to zero,

$$i_{rq} = -\frac{L_m}{L_r}i_{sq} \tag{3.3.5}$$

The constant alignment of the d-axis with $\vec{\lambda}_r$, results in $\lambda_{rq}$ being zero, similarly guarantees that $\frac{d}{dt}\lambda_{rq}$ $is\,also\,zero.\frac{L_r}{R_r}\frac{d}{dt}\lambda_r + \lambda_r = L_m$ (3.3.6) In a squirrel-cage rotor with $v_{rq} = 0$,

$$\omega_{sl} = -\frac{R_r}{\lambda_r}i_{rq} \tag{3.3.7}$$

Substituting value of $i_{rq}$ from eq.14 we get:

$$\omega_{sl} = \frac{L_m R_r}{\lambda_r L_r}i_{sq} \tag{3.3.8}$$

The developed electromechanical torque is defined as:

$$T_{em} = \frac{3}{2}\frac{p}{2}\frac{L_m}{L_r}\lambda_r i_{sq} \tag{3.3.9}$$

# Controller Design

Because of the dynamic system's non-minimum phase behaviour, it is challenging to control the DC bus voltage at the DC bus to the necessary level. A phenomenon known as "non-minimum phase behaviour" occurs when the system deviates in the opposite direction for a while before finally converging in the correct direction. Moreover, there are intrinsic physical restrictions that place limits on the controllable state for these non-minimum phase systems.

To run the system as quickly as possible, either the non-minimum phase behaviour is minimized or a control mechanism is created to offset this behaviour. Here is how an indirect methodology based on the power balance equation is put into practice.

$$P_{in} = P_{out} \tag{4.0.1}$$

$$P_{fc} + P_{bat} + P_{sc} + P_{pv} = P_{out} \tag{4.0.2}$$

Where $P_{fc}$,$P_{bat}$,$P_{sc}$ and $P_{pv}$ represent powers of FC,battery,SC and PV respectively.Solving equation(27) to get $x_{1ref}$ we have,

$$x_{1ref} = \omega \left( \frac{P_{out} - P_{bat} - P_{sc} - P_{pv}}{v_{fc}} \right) \tag{4.0.3}$$

where $\omega$ is a constant that represents various power losses, such as power loss due to inductances.

## 4.1   Sliding mode controller

SMC, a non-linear variable structure control technique, aids in achieving system trajectory stability.A controller is created to help the system reach its target value by guiding the model to-

wards the drawn sliding surface.A system state with a starting value reaches the sliding surface by the use of control law, and after that, the state reaches the intended value.

### 4.1.1 SMC for HESS

In order to track all states to their intended values, the following error words are defined:

$$e_1 = y_1 - y_{1ref} \tag{4.1.1}$$

$$e_2 = y_2 - y_{2ref} \tag{4.1.2}$$

$$e_3 = y_3 - y_{3ref} \tag{4.1.3}$$

$$e_4 = y_4 - y_{4ref} \tag{4.1.4}$$

$y_{1ref}, y_{2ref}, y_{3ref}$ and $y_{4ref}$ are the refernce values of FC,battery,SC and PV currents,Taking time derivative of error terms: $\dot{y}_1, \dot{y}_2, \dot{y}_3$ and $\dot{y}_4$ from Eqs.(29)-(32),we get:

$$\dot{e}_1 = \dot{y}_1 - \dot{y}_{1ref} \tag{4.1.5}$$

$$\dot{e}_2 = \dot{y}_2 - \dot{y}_{2ref} \tag{4.1.6}$$

$$\dot{e}_3 = \dot{y}_3 - \dot{y}_{3ref} \tag{4.1.7}$$

$$\dot{e}_4 = \dot{y}_4 - \dot{y}_{4ref} \tag{4.1.8}$$

Putting values of $\dot{y}_1, \dot{y}_2, \dot{y}_3$ and $\dot{y}_4$ from Eqs.(1)-(4),we get:

$$\dot{e}_1 = \frac{v_{fc}}{L_1} - \frac{R_1 y_1}{L_1} - \frac{y_5(1-a_1)}{L_1} - \dot{y}_{1ref} \tag{4.1.9}$$

$$\dot{e}_2 = \frac{v_{bat}}{L_2} - \frac{R_2 y_2}{L_2} - \frac{y_5 a_{23}}{L_2} - \dot{y}_{2ref} \tag{4.1.10}$$

$$\dot{e}_3 = \frac{v_{sc}}{L_3} - \frac{R_3 y_3}{L_3} - \frac{y_5 a_{45}}{L_3} - \dot{y}_{3ref} \tag{4.1.11}$$

$$\dot{e}_4 = \frac{v_{pv}}{L_4} - \frac{R_4 y_4}{L_4} - \frac{y_5(1-a_6)}{L_4} - \dot{y}_{4ref} \tag{4.1.12}$$

In general sliding surface for MIMO system is defined as:

$$S = [S_1, S_2, ..., S_n]^T \tag{4.1.13}$$

For the corresponding control inputs, four sliding surfaces $S_1$, $S_2$, $S_3$, and $S_4$ are defined as follows:

$$S_1 = c_1 e_1 \tag{4.1.14}$$

$$S_2 = c_2 e_2 \tag{4.1.15}$$

$$S_3 = c_3 e_3 \tag{4.1.16}$$

$$S_4 = c_4 e_4 \tag{4.1.17}$$

where c1, c2, c3 and c4 are positive constants. Taking time derivative of Eqs. (42)-(45) and substituting the values of $\dot{e}_1$ , $\dot{e}_2$ , $\dot{e}_3$ and $\dot{e}_4$ from Eqs. (37)-(40), we get,

$$\dot{S}_1 = c_1 \left( \frac{v_{fc}}{L_1} - \frac{R_1 y_1}{L_1} - \frac{y_5(1-a_1)}{L_1} - \dot{y}_{1ref} \right) \tag{4.1.18}$$

$$\dot{S}_2 = c_2 \left( \frac{v_{bat}}{L_2} - \frac{R_2 y_2}{L_2} - \frac{y_5 a_{23}}{L_2} - \dot{y}_{2ref} \right) \tag{4.1.19}$$

$$\dot{S}_3 = c_3 \left( \frac{v_{sc}}{L_3} - \frac{R_3 y_3}{L_3} - \frac{y_5 a_{45}}{L_3} - \dot{y}_{3ref} \right) \tag{4.1.20}$$

$$\dot{S}_4 = c_4 \left( \frac{v_{pv}}{L_4} - \frac{R_4 y_4}{L_4} - \frac{y_5(1-a_6)}{L_4} - \dot{y}_{4ref} \right) \tag{4.1.21}$$

In order to perform stability analysis and to determine the desired dynamics of the damping term,consider following Lyapunov candidate function

$$V = \frac{S_1^2}{2} + \frac{S_2^2}{2} + \frac{S_3^2}{2} + \frac{S_4^2}{2} \tag{4.1.22}$$

$$\dot{V} = S_1 \dot{S}_1 + S_2 \dot{S}_2 + S_3 \dot{S}_3 + S_4 \dot{S}_4 \tag{4.1.23}$$

Putting the values of $\dot{S}_1$ , $\dot{S}_2$ , $\dot{S}_3$ and $\dot{S}_4$ from Eqs. (38)-(41) in above Eq. (43), we get,

$$\dot{V} = S_1 \left[ c_1 \left( \frac{v_{fc}}{L_1} - \frac{R_1 y_1}{L_1} - \frac{y_5(1-a_1)}{L_1} - \dot{y}_{1ref} \right) \right]$$

$$+ S_2 \left[ c_2 \left( \frac{v_{bat}}{L_2} - \frac{R_2 y_2}{L_2} - \frac{y_5 a_{23}}{L_2} - \dot{y}_{2ref} \right) \right]$$

$$+ S_3 \left[ c_3 \left( \frac{v_{sc}}{L_3} - \frac{R_3 y_3}{L_3} - \frac{y_5 a_{45}}{L_3} - \dot{y}_{3ref} \right) \right]$$

$$+ S_4 \left[ c_4 \left( \frac{v_{pv}}{L_4} - \frac{R_4 y_4}{L_4} - \frac{y_5(1-a_6)}{L_4} - \dot{y}_{4ref} \right) \right]$$

(4.1.24)

To meet the Lyapunov stability criterion, which requires

$\dot{V} \le 0$, consider, the following constraints,

$$-A_1 |S_1|^\alpha \operatorname{sign}\left(\tfrac{S_1}{\rho_1}\right) = \frac{c_1 v_{fc}}{L_1} - \frac{c_1 R_1 y_1}{L_1} - \frac{c_1 y_5(1-a_1)}{L_1}$$
$$- c_1 \dot{y}_{1ref}$$

(4.1.25)

$$-A_2 |S_2|^\beta \operatorname{sign}\left(\tfrac{S_2}{\rho_2}\right) = \frac{c_2 v_{bat}}{L_2} - \frac{c_2 R_2 y_2}{L_2} - \frac{c_2 y_5 a_{23}}{L_2}$$
$$- c_2 \dot{y}_{2ref}$$

(4.1.26)

$$-A_3 |S_3|^\gamma \operatorname{sign}\left(\tfrac{S_3}{\rho_3}\right) = \frac{c_3 v_{sc}}{L_3} - \frac{c_3 R_3 y_3}{L_3} - \frac{c_3 y_5 a_{45}}{L_2}$$
$$- c_3 \dot{y}_{3ref}$$

(4.1.27)

$$-A_4 |S_4|^\zeta \operatorname{sign}\left(\tfrac{S_4}{\rho_4}\right) = \frac{c_4 v_{pv}}{L_4} - \frac{c_4 R_4 y_4}{L_4} - \frac{c_4 y_5(1-a_6)}{L_4}$$
$$- c_4 \dot{y}_{4ref}$$

(4.1.28)

we considered $\dot{s}_i = -A_i |S_i|^\zeta \operatorname{sign}\left(\tfrac{S_i}{\rho_i}\right)$ This is the Sliding Mode Control (SMC) technique's reaching law.It accelerates the rate of convergence when the system state is far from the switching manifold and is known as the power rate reaching law.where the constant design parameters A1, A2, A3, and A4 (controller gains) have positive values.

$S_i^\alpha$, $S_i^\beta$, $S_i^\gamma$ The system's convergence to the sliding surfaces is ensured by ,$|S_i|^\zeta$. Positive constants $\alpha$, $\beta$, $\gamma$, and $\zeta$ are frequently chosen from the range of 0 to 1.The chattering effect is lessened by $\rho_1$, $\rho_2$, $\rho_3$, and $\rho_4$.We define the signum function as follows:

$$sign(y) = \begin{cases} -1, & \text{if } S_i < 0 \\ 0, & \text{if } S_i = 0 \\ 1, & \text{if } S_i > 0 \end{cases}$$

(4.1.29)

17

Where i = 1, 2, 3, 4.Now solving the Eqs for control inputs $a_1, a_{23}, a_{45}$ and $a_6$ we get:

$$a_1 = \frac{L_1}{c_1 y_5} \left[ \frac{c_1 R_1 y_1}{L_1} - \frac{c_1 v_{fc}}{L_1} + \frac{c_1 y_5}{L_1} + c_1 \dot{y}_{1ref} \right.$$
$$\left. -A_1 |S_1|^\alpha \operatorname{sign}\left(\frac{S_1}{\rho_1}\right) \right]$$

(4.1.30)

$$a_{23} = \frac{L_2}{c_2 y_5} \left[ -\frac{c_2 R_2 y_2}{L_2} + \frac{c_2 v_{bat}}{L_2} - c_2 \dot{y}_{2ref} \right.$$
$$\left. +A_2 |S_2|^\beta \operatorname{sign}\left(\frac{S_2}{\rho_2}\right) \right]$$

(4.1.31)

$$a_{45} = \frac{L_3}{c_3 y_5} \left[ -\frac{c_3 R_3 y_3}{L_3} + \frac{c_3 v_{sc}}{L_3} - c_3 \dot{y}_{3ref} \right.$$
$$\left. +A_3 |S_3|^\gamma \operatorname{sign}\left(\frac{S_3}{\rho_3}\right) \right]$$

(4.1.32)

$$a_6 = \frac{L_4}{c_4 y_5} \left[ \frac{c_4 R_4 y_4}{L_4} - \frac{c_4 v_{pv}}{L_4} + \frac{c_4 y_5}{L_4} + c_4 \dot{y}_{4ref} \right.$$
$$\left. -A_4 |S_4|^\zeta \operatorname{sign}\left(\frac{S_4}{\rho_4}\right) \right]$$

(4.1.33)

In order to prove stability ,the time derivative of Lyapunov function can be written as follows:

$$\dot{V} = -S_1 A_1 |S_1|^\alpha \operatorname{sign}\left(\frac{S_1}{\rho_1}\right)$$
$$-S_2 A_2 |S_2|^\beta \operatorname{sign}\left(\frac{S_2}{\rho_2}\right)$$
$$-S_3 A_3 |S_3|^\gamma \operatorname{sign}\left(\frac{S_3}{\rho_3}\right)$$
$$-S_4 A_4 |S_4|^\zeta \operatorname{sign}\left(\frac{S_4}{\rho_4}\right)$$

(4.1.34)

By taking into account the properties of the sign(.) function defined in above equation can be simplified as

$$\dot{V} = -S_1 A_1 |S_1|^\alpha \operatorname{sign}\left(\frac{S_1}{\rho_1}\right)$$
$$-S_2 A_2 |S_2|^\beta \operatorname{sign}\left(\frac{S_2}{\rho_2}\right)$$
$$-S_3 A_3 |S_3|^\gamma \operatorname{sign}\left(\frac{S_3}{\rho_3}\right)$$
$$-S_4 A_4 |S_4|^\zeta \operatorname{sign}\left(\frac{S_4}{\rho_4}\right) \leq 0$$

(4.1.35)

The sliding mode controller satisfies the stability requirements, which guarantee the stability of the system and the convergence of errors to zero within a finite amount of time, as shown by a Lyapunov stability analysis.

## 4.1.2  SMC for Induction Motor

The stator d and q axis voltages can be defined as follows:

$$v_{sd} = R_s i_{sd} + \sigma L_s \frac{d}{dt} \beta_{sd} + \frac{L_m}{L_r} \frac{d}{dt} \lambda_{rd} - \omega_d \sigma L_s i_{sq} \tag{4.1.36}$$

$$v_{sq} = R_s i_{sq} + \sigma L_s \frac{d}{dt} \beta_{sq} + \omega_d \frac{L_m}{L_r} \frac{d}{dt} \lambda_{rd} - \omega_d \sigma L_s i_{sd} \tag{4.1.37}$$

In Eqs. (4.1.36) only the first two terms on the right are due to the d-axis current $i_{sd}$ and $\frac{d}{dt}\beta_{sd}$
. Other terms are resulting from $\lambda_{rd}$ and $i_{sq}$ may be considered disturbances.Likewise, in Eqs.
(4.1.37), the terms due to $\lambda_{rd}$ and $i_{sd}$ can be considered as disturbances.  Therefore, these equations can be rewritten as:

$$v_{sd} = R_s i_{sd} + \sigma L_s \frac{d}{dt} \beta_{sd} \tag{4.1.38}$$

$$v_{sq} = R_s i_{sq} + \sigma L_s \frac{d}{dt} \beta_{sq} \tag{4.1.39}$$

PI controllers are implemented in the speed as well as current loops in [1].For speed loop,PI controller gains are calculated with the phase margin of 60 and the open loop crossover frequency of 25 rad/s.In order to calculate the gains associated with the proportional and integral components of the PI controllers for current loops, it is assumed that the compensation is perfect.Hence, each channel will result in a block diagram shown. Reference voltages for $V_{sd}$ and $V_{sq}$ are calculated using stator dq-axis reference current,$i_{sd}$,$i_{sq}$,$\lambda_{rd}$ and $\omega_d$.The actual stator voltages $V_a$, $V_b$, and $V_c$ are supplied by the power electronics converter,using the stator voltage space vector modulation technique.  The mechanical speed equation of an induction motor is commonly represented as follows:

$$\dot{\omega}_{mech1} = \frac{T_{em} - T_l}{J_{eq}} \tag{4.1.40}$$

where J is the inertia constant, $T_l is the external load, p is the pole numbers, and T_em$ is the generated torque of an induction motor. putting the value of $T_em$

$$\dot{\omega}_{mech} = \frac{\frac{3}{2} \frac{p}{2} \frac{L_m}{L_r} \lambda_r i_{sq} - T_l}{J_{eq}} \tag{4.1.41}$$

simplifying above equation we get:

$$\dot{\omega}_{mech} = b i_{sq} - f \tag{4.1.42}$$

Where $b = \frac{3}{2} \frac{p}{2} \frac{L_m}{L_r} \frac{\lambda_r}{J_{eq}}$ and $f = \frac{T_l}{J_{eq}}$

$$e_5 = \omega_{mech} - \omega_{mechref} \tag{4.1.43}$$

$$\dot{e}_5 = \dot{\omega}_{mech} - \dot{\omega}_{mechref} \qquad (4.1.44)$$

Putting values of $\dot{\omega}_{mech}$

$$\dot{e}_5 = bi_{sq} - f - \dot{\omega}_{mechref} \qquad (4.1.45)$$

Then the sliding surface can be defined as:

$$S_5 = c_5 e_5 \qquad (4.1.46)$$

Taking time derivative of above Eq.:

$$\dot{S}_1 = c_5 \dot{e}_5 \qquad (4.1.47)$$

Replacing the value of $\dot{e}_5$ from Eqs. (77), we get:

$$\dot{S}_5 = c_5 \left( bi_{sq} - f - \dot{\omega}_{mechref} \right) \qquad (4.1.48)$$

Lyapunov candidate function is given as follows:

$$V = \frac{S_5^2}{2} \qquad (4.1.49)$$

$$\dot{V} = S_5 \dot{S}_5 \qquad (4.1.50)$$

Putting the values of $\dot{S}_1$

$$\dot{V} = S_5 \left[ c_5 \left( bi_{sq} - f - \dot{\omega}_{mechref} \right) \right] \qquad (4.1.51)$$

To prove stability of the system ,$\dot{S}_1$ can be replaced by following parameters

$$\dot{S}_5 = -A_5 |S_5|^\delta \, \text{sign} \left( \frac{S_5}{0.5} \right) \qquad (4.1.52)$$

To meet condition of $\dot{V} \leq 0$ , consider the following constraints,

$$c_5 bi_{sq} - c_5 f - c_5 \dot{\omega}_{mechref} = -A_5 |S_5|^\delta \, \text{sign} \left( \frac{S_5}{0.5} \right) \qquad (4.1.53)$$

Nothe control input $i_{sq}$, we obtain:

$$i_{sq} = \frac{1}{c_5 b} \left( -A_5 |S_5|^\delta \, \text{sign} \left( \frac{A_5}{0.5} \right) + c_5 f + c_5 \dot{\omega}_{mechref} \right) \qquad (4.1.54)$$

$$\dot{V} = -S_5 A_5 |S_5|^\delta \, \text{sign} \left( \frac{S_1}{\rho_1} \right) \qquad (4.1.55)$$

$$\dot{V} = -S_5 A_5 |S_5|^\delta \, \text{sign} \left( \frac{S_1}{\rho_1} \right) \leq 0 \qquad (4.1.56)$$

## 4.2 Barrier Function based Adaptive Sliding mode controller

$$\dot{y}(t) = u(t) + \delta(t) \tag{4.2.1}$$

where $\delta(t)$ is the system's disturbance.The function $\delta(t)$ is a bounded function with an unknown upper bound, i.e. $|\delta(t)| \leq \delta_{\text{max}}$.However, there is a positive bound $\delta_{\text{max}}$ whose exact value is unknown. The output of the system is represented by $y(t) in mathbbR$. A first-order sliding mode controller is necessary to achieve system stability, which is represented as:

$$u(t) = -A(t)sign(y) \tag{4.2.2}$$

Sliding mode control ensures finite-time convergence and closed-loop insensitivity to disturbances. Understanding the top bound of disturbances is required to develop first-order sliding mode controllers (FOSMCs). This limit is frequently unknown. This is a significant barrier in the installation of FOSMCs, resulting in unwanted chattering.

The first adaptation method is increasing gain until the SM is reached, then fixing it at this value to maintain an optimal SM for a predetermined period of time.As the number of disturbances increases, the SM may be lost, necessitating an increase in gain to reclaim it.

However, utilising this technique overestimates FOSMC gain and cannot guarantee that the SM will not be lost in the future. To overcome this issue, an approach based on rising and reducing gain has been proposed. This strategy ensures that the sliding variable converges near zero in finite time while not overestimating the gain. The primary problem with this technique is that the size of the neighbourhood and convergence time are dependent on the unknown upper bound of the disturbance, making it impossible to ensure that SM will not be lost for longer values of time.

The second adaptation strategy uses the comparable control value to estimate disturbances.A low-pass filtered approximation of the similar control was proposed as a way to implement this method. During implementation, make sure to select a filter constant that is less than the inverse of the upper bound of the first derivative of the disturbance.

Furthermore, adaptive SMC based on barrier functions can be used to alleviate both of the above mentioned problems. Equation (4.2.1) demonstrates that the control rule is a function of the system's state and varies with time.To define the barrier functions, two unique ways are proposed in this study. Consider some fixed $\phi > 0$ then BF is defined as an even continuous function $A_b : x \in [-\phi, \phi[ \rightarrow A_b(x) \in [b, \infty[$ strictly growing on $[0, \phi[$
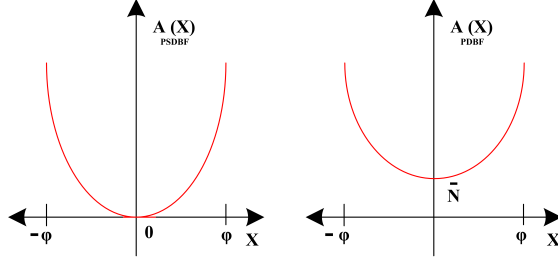
**Figure 4.1:** Barrier Function

- **Positive definite barrier function(PBF):**

$$A_{p,b}(x) = \frac{\overline{\phi}N}{\phi - |x|}, \quad A_{p,b}(0) = \overline{N} > 0 \tag{4.2.3}$$

- **Positive semi definite barrier function(PSBF):**

$$A_{p,b}(x) = \frac{|x|}{\phi - |x|}, \quad A_{p,b}(0) = 0 \tag{4.2.4}$$

When $\phi \to 0$, then $A \to 0$. When the output variable is in vicinity of origin,i.e., $\frac{|x|}{\phi} < 1$, then $A \approx \frac{|x|}{\phi}$, and this guarantees the convergence of state $x$ to zero.

### 4.2.1 Barrier function based ASMC for HESS

Defining errors for stable working of the HESS system,

$$S_1 = y_1 - y_{1ref} \tag{4.2.5}$$

$$S_2 = y_2 - y_{2ref} \tag{4.2.6}$$

$$S_3 = y_3 - y_{3ref} \tag{4.2.7}$$

$$S_4 = y_4 - y_{4ref} \tag{4.2.8}$$

The derivative of above eqs.(4.2.5)-(4.2.8) and subtituting the values of $\dot{y}_1, \dot{y}_2, \dot{y}_3$ and $\dot{y}_4$ we obtain,

$$\dot{S}_1 = \frac{v_{fc}}{L_1} - \frac{R_1 y_1}{L_1} - \frac{y_5(1-a_1)}{L_1} - \dot{y}_{1ref} + \theta_1 \tag{4.2.9}$$

$$\dot{S}_2 = \frac{v_{bat}}{L_2} - \frac{R_2 y_2}{L_2} - \frac{y_5 a_{23}}{L_2} - \dot{y}_{2ref} + \theta_2 \tag{4.2.10}$$

$$\dot{S}_3 = \frac{v_{sc}}{L_3} - \frac{R_3 y_3}{L_3} - \frac{y_5 a_{45}}{L_3} - \dot{y}_{3ref} + \theta_3 \tag{4.2.11}$$

$$\dot{S}_4 = \frac{v_{pv}}{L_4} - \frac{R_4 y_4}{L_4} - \frac{y_5(1 - a_6)}{L_4} - \dot{y}_{4ref} + \theta_4 \tag{4.2.12}$$

In above equations $\theta_1, \theta_2, \theta_3$ and $\theta_4$ are untied bounds, and the controller attempts to adaptively reduce these factors. The following equations can be obtained by solving eqs.(93)-(96) for $a_1, a_{23}, a_{45}$, and $a_6$,

$$a_1 = \frac{L_1}{y_5} \left( \frac{R_1 y_1}{L_1} - \frac{v_{fc}}{L_1} + \frac{y_5}{L_1} + \dot{y}_{1ref} + \dot{S}_1 \right) \tag{4.2.13}$$

$$a_{23} = \frac{L_2}{y_5} \left( -\frac{R_2 y_2}{L_2} + \frac{v_{bat}}{L_2} - \dot{y}_{2ref} + \dot{S}_2 \right) \tag{4.2.14}$$

$$a_{45} = \frac{L_3}{y_5} \left( -\frac{R_3 y_3}{L_3} + \frac{v_{sc}}{L_3} - \dot{y}_{3ref} + \dot{S}_3 \right) \tag{4.2.15}$$

$$a_6 = \frac{L_4}{y_5} \left( \frac{R_4 y_4}{L_4} - \frac{v_{pv}}{L_4} + \frac{y_5}{L_4} + \dot{y}_{4ref} + \dot{S}_4 \right) \tag{4.2.16}$$

BF for $\dot{S}_1, \dot{S}_2, \dot{S}_3$ and $\dot{S}_4$ can be given as,

$$\dot{S}_1 = -A_1 |S_1| \operatorname{sign}(S_1) \tag{4.2.17}$$

$$\dot{S}_2 = -A_2 |S_2| \operatorname{sign}(S_2) \tag{4.2.18}$$

$$\dot{S}_3 = -A_3 |S_3| \operatorname{sign}(S_3) \tag{4.2.19}$$

$$\dot{S}_4 = -A_4 |S_4| \operatorname{sign}(S_4) \tag{4.2.20}$$

In above eqs.$A_1, A_2, A_3$, and $A_4$ are adaptive gains. followings eqs. are obtained after solving above equations,,

$$a_1 = 1 + \frac{L1}{y5} \left( \frac{y1}{R1L1} - \frac{v_{fc}}{L1} + \dot{y}_{1ref} - A_1 |S_1| \operatorname{sign}(S_1) \right) \tag{4.2.21}$$

$$a_{23} = \frac{L2}{y5} \left( -\frac{y2}{R2L2} + \frac{v_{bat}}{L2} - \dot{y}_{2ref} + A_2 |S_2| \operatorname{sign}(S_2) \right) \tag{4.2.22}$$

$$a_{45} = \frac{L3}{y5} \left( -\frac{y3}{R3L3} + \frac{v_{sc}}{L3} - \dot{y}_{3ref} + A_3 |S_3| \operatorname{sign}(S_3) \right) \tag{4.2.23}$$

$$a_6 = 1 + \frac{L4}{y5} \left( \frac{y4}{R4L4} - \frac{vpv}{L4} + \dot{y}_{4\text{ref}} - A_4|S_4|\operatorname{sign}(S_4) \right) \tag{4.2.24}$$

There exists $\bar{t}$, the smallest root of the equation $|S(t)| \leq \phi^2$, for any $S(0)$ and $\phi > 0$, such that for all $t \geq \bar{t}$, the inequality $|S(t)| < \phi$ holds.Hence, the proposed controller is stable, is also explained using the Lyapunov stability equations. Following Lyapunov candidate function is considered for the stability analysis of controller,

$$V(S(t), A(S(t))) = \frac{1}{2}S^2(t) + \frac{1}{2}(A(S(t)) - A(0))^2 \tag{4.2.25}$$

Taking the time derivative of above eq. we get,

$$\dot{V}(S(t), A(S(t))) \leq -\sigma V^{\frac{1}{2}}(S(t), A(S(t))) \tag{4.2.26}$$

where $\sigma > 0$, $V^{\frac{1}{2}}(S(t), A(S(t))) \geq 0$, so eq. (110) can be written as,

$$\dot{V}(S(t), A(S(t))) \leq 0 \tag{4.2.27}$$

### 4.2.2 Barrier Function based ASMC for Induction Motor

For stable working of induction motor,speed error can be defined as,

$$s_5 = \omega_{mech} - \omega_{mechref} \tag{4.2.28}$$

$$\dot{s}_5 = \dot{\omega}_{mech} - \dot{\omega}_{mechref} \tag{4.2.29}$$

$$\dot{s}_5 = bi_{sq} - f - \dot{\omega}_{mechref} \tag{4.2.30}$$

$$\dot{S}_5 = bi_{sq} - f - \dot{\omega}_{mechref} + \theta_5 \tag{4.2.31}$$

$$i_{sq} = \frac{1}{b}(\dot{S}_5 + f + \dot{\omega}_{mechref}) \tag{4.2.32}$$

$$\dot{S}_5 = -A_5|S_5|\operatorname{sign}(S_5) \tag{4.2.33}$$

$$i_{sq} = \frac{1}{b}\left( -A_5|S_5|\operatorname{sign}(S_5) + f + \dot{\omega}_{mechref} \right) \tag{4.2.34}$$

For stability analysis,following Lyapunov candidate function is used which has both output variable and adaptice gain,

$$V(S(t), A(S(t))) = \frac{1}{2}S^2(t) + \frac{1}{2}(A(S(t)) - A(0))^2 \tag{4.2.35}$$

Taking the time derivative of above eq. we get,

$$\dot{V}(S(t), A(S(t))) \leq -\zeta V^{\frac{1}{2}}(S(t), A(S(t))) \qquad (4.2.36)$$

where $\zeta > 0$, $V^{\frac{1}{2}}(S(t), A(S(t))) \geq 0$, so eq. (4.2.36) can be written as,

$$\dot{V}(S(t), A(S(t))) \leq 0 \qquad (4.2.37)$$

CHAPTER 5

# Discussion

## 5.1 Simulation Results

MATLAB/Simulink® (2022a) was used in this section to simulate and evaluate the proposed/designed controller under various load circumstances.The suggested model's major purpose is to regulate the DC bus voltage, control the current flow by creating reference current for the power sources, and provide precise speed reference tracking.After comparing the error results in Table 5.4-5.5, it is concluded tha barrier function based adaptive sliding mode controller is seen as superior to the other controllers.Table 5.1 shows the parameters of the DC-DC converters used in this study.Similarly Table 5.3 shows Controller parameters used for tuning controllers.

**Table 5.1:** Parameters of DC-DC convereters

| Parameters | Values |
|---|---|
| Inductances $L_1$,$L_2$,$L_3$ and $L_4$ | 3.3 mH |
| Resistances $R_1$,$R_2$,$R_3$ and $R_4$ | 20 mΩ |
| Capacitances $C_1$ and $C_2$ | 1.66 mF |
| constant($\omega$) | 1.0004 |

## 5.2 Real Time Results

The MATLAB/Simulink simulations results indicated that BFASMC controller responded effi-ciently under variable load conditions. The same system and controller's reaction is now vali-
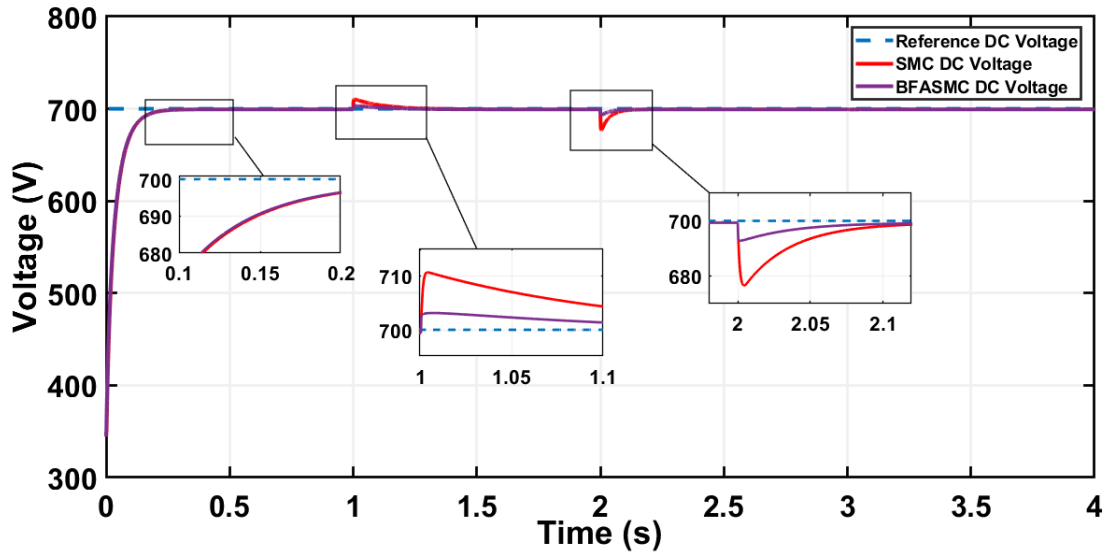
**Figure 5.1:** Comparison plot of DC Bus Voltage (SMC vs BFASMC).
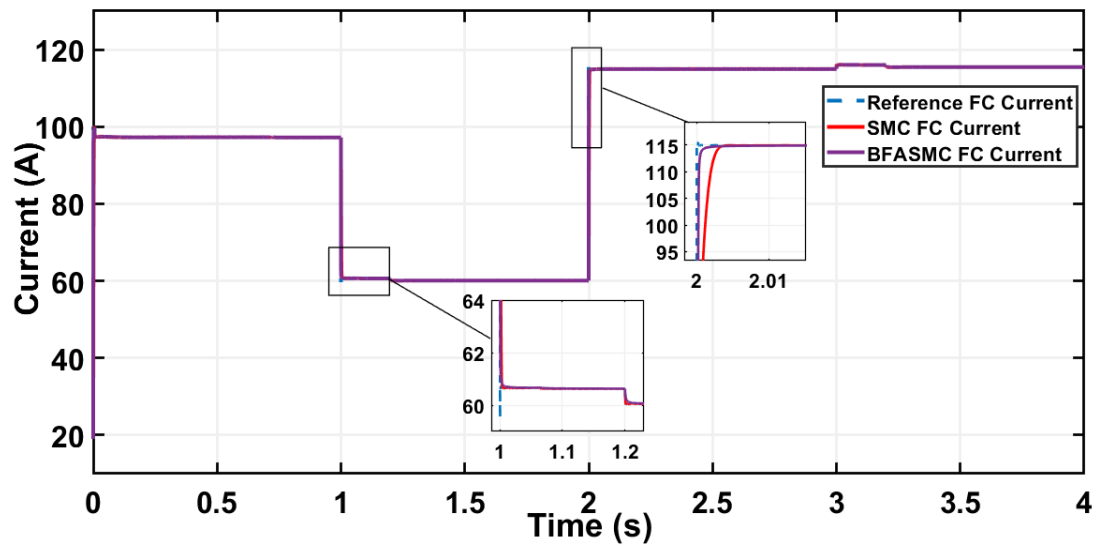


**Figure 5.2:** Comparative graph of FC current (SMC vs BFASMC).
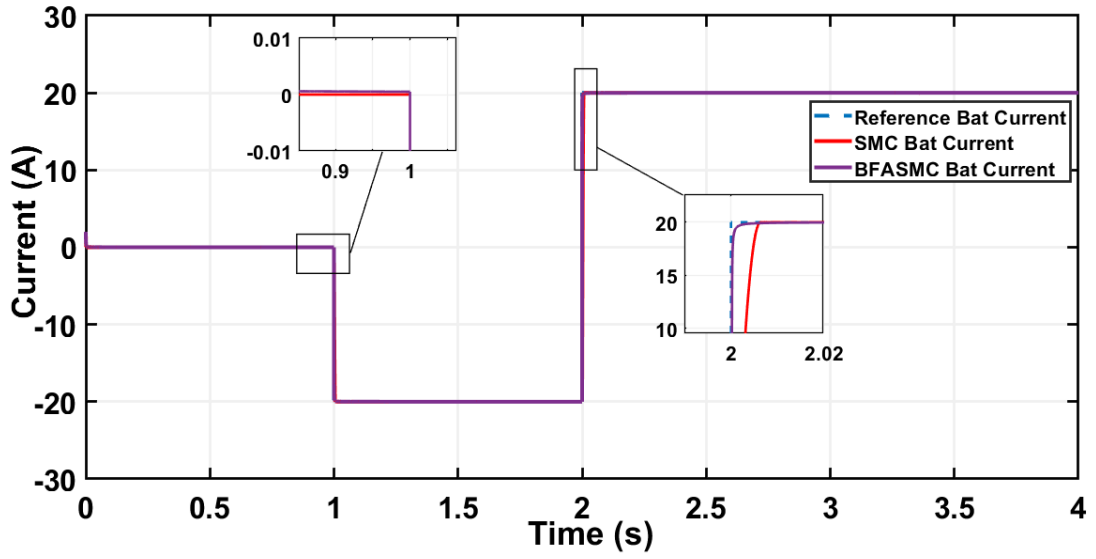
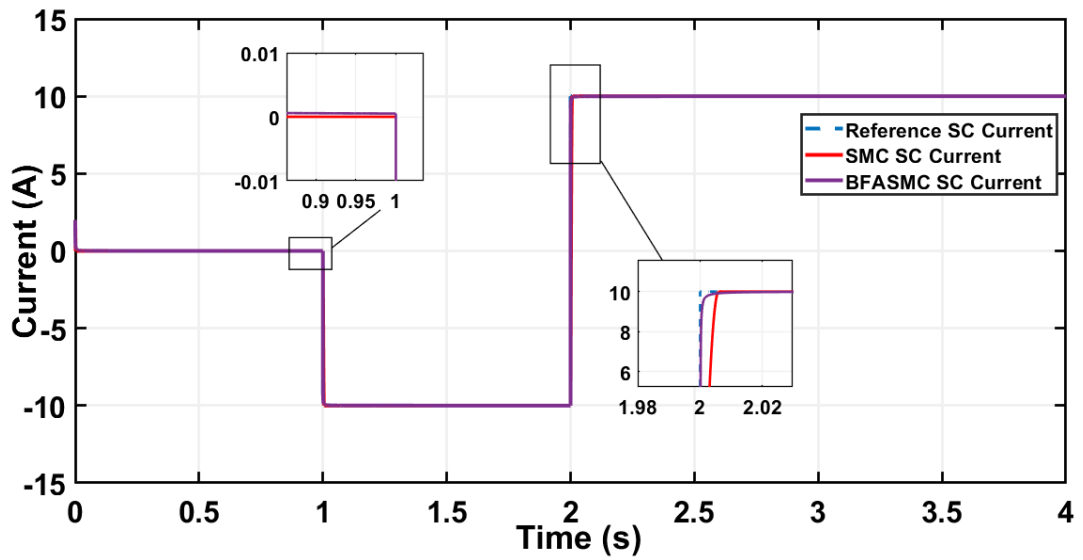**Figure 5.3:** Comparative graph of Battery current (SMC vs BFASMC).



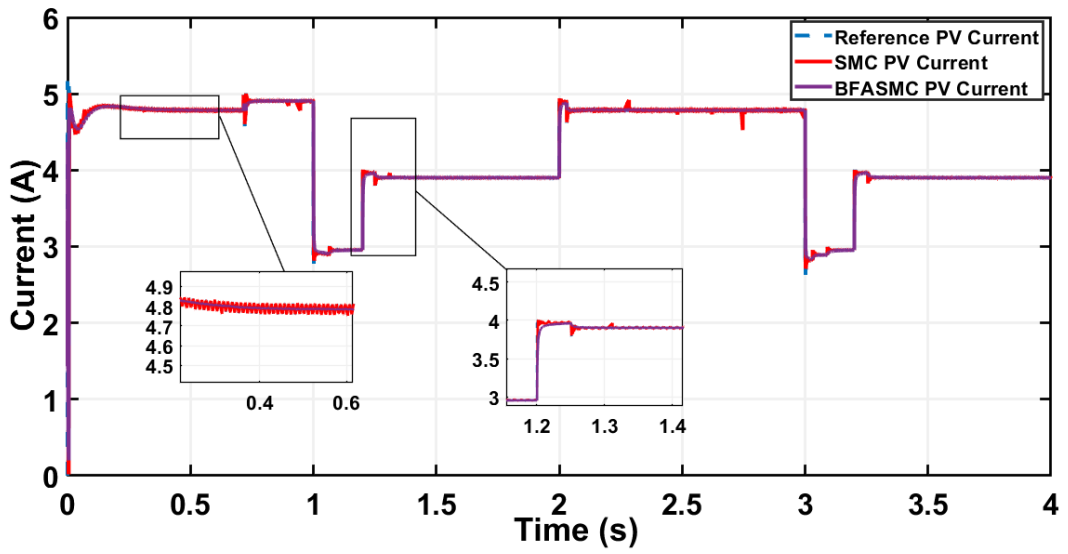**Figure 5.4:** Comparative graph of SC current (SMC vs BFASMC).

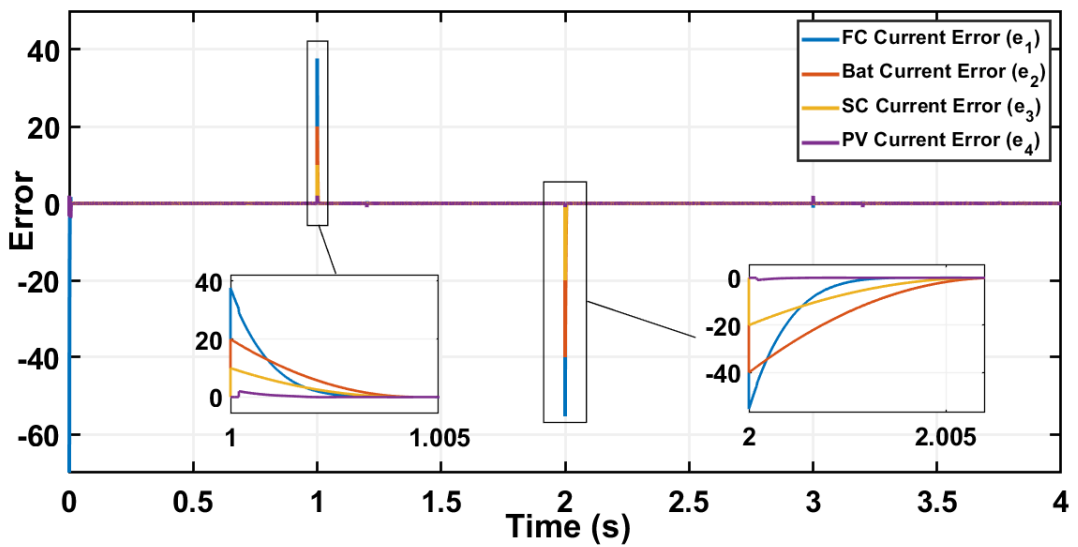**Figure 5.5:** Comparative graph of PV current (SMC vs BFASMC).



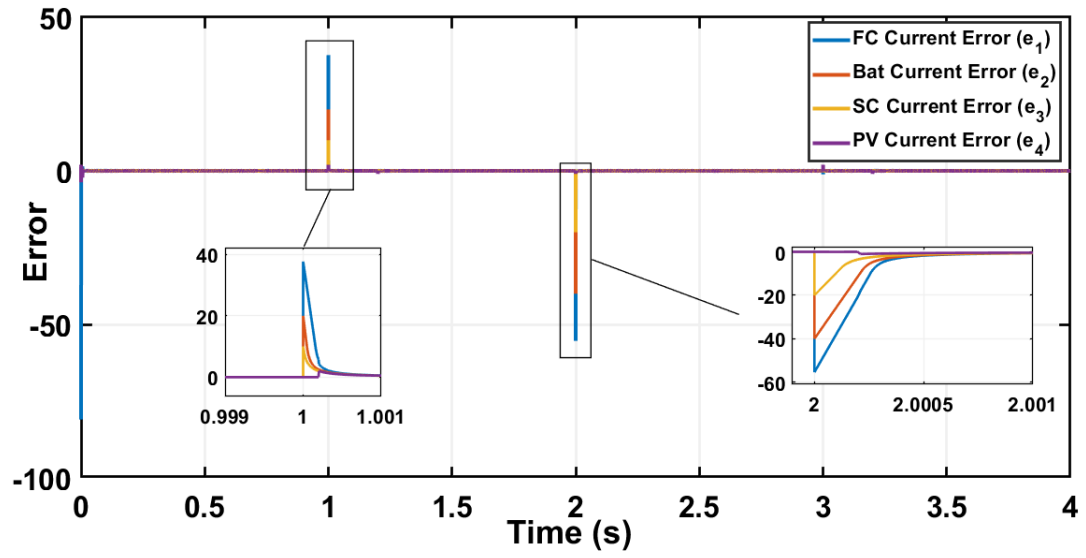**Figure 5.6:** Tracking errors of source currents using SMC.
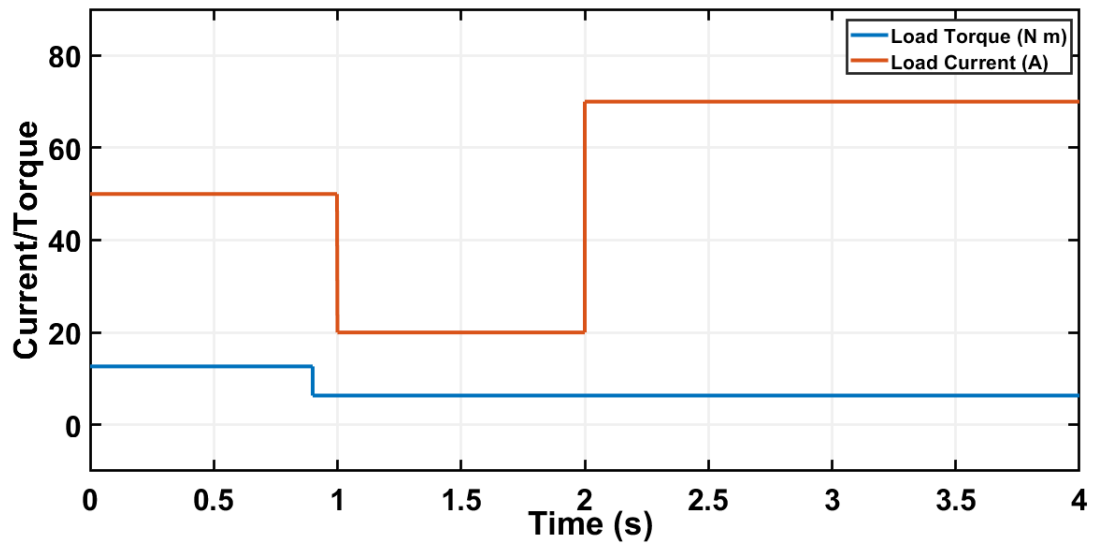
**Figure 5.7:** Tracking errors of source currents using BFASMC.
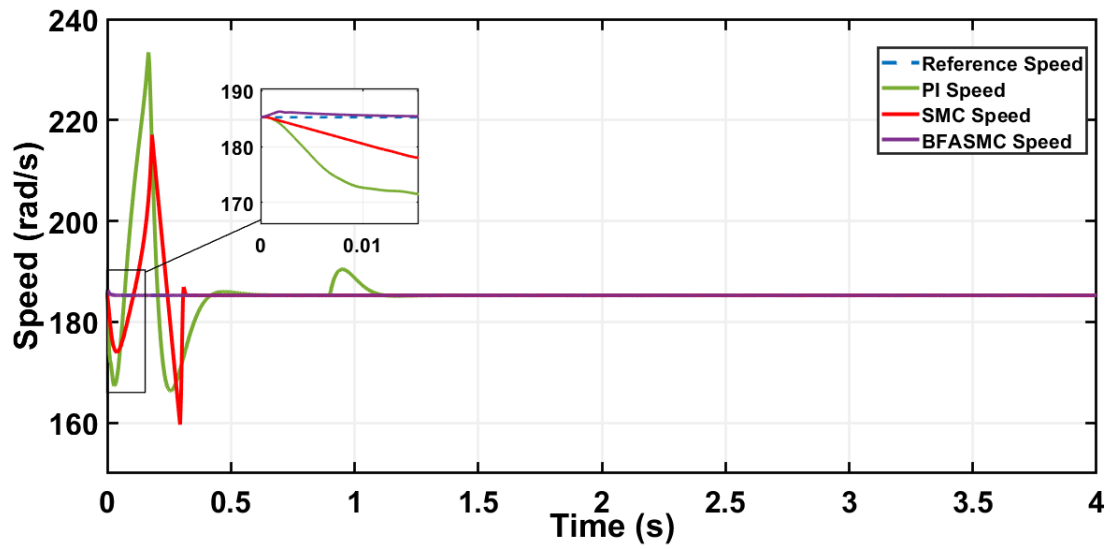


**Figure 5.8:** Load current and load torque profile.

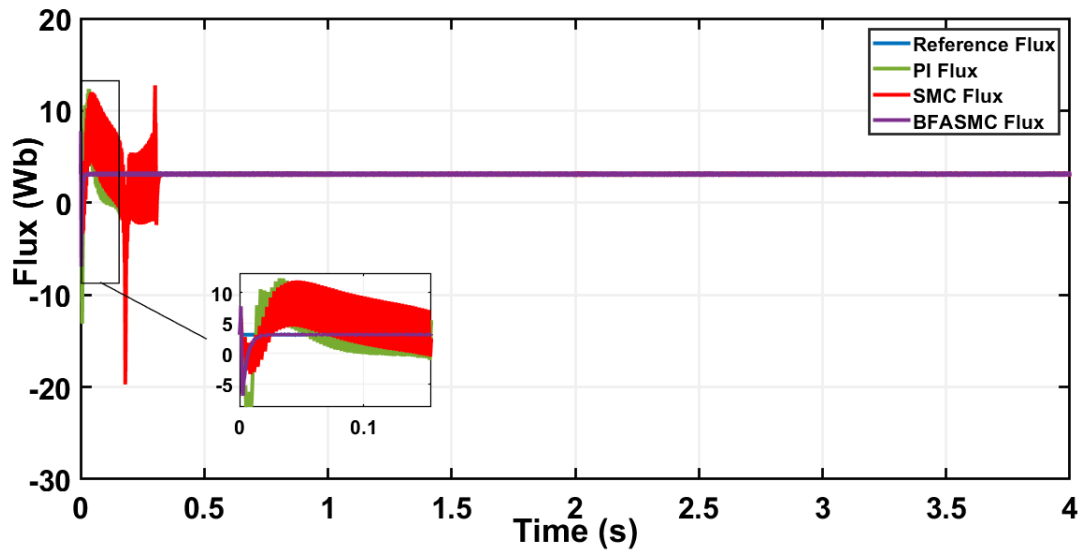**Figure 5.9:** Comparative graph of speed (PI vs SMC vs BFASMC).



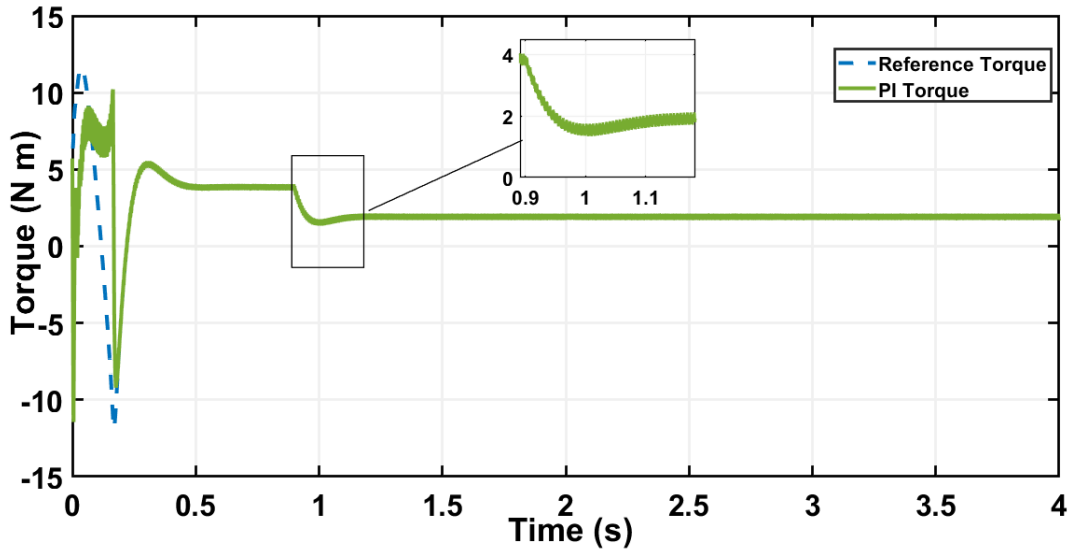**Figure 5.10:** Comparative graph of flux (PI vs SMC vs BFASMC).
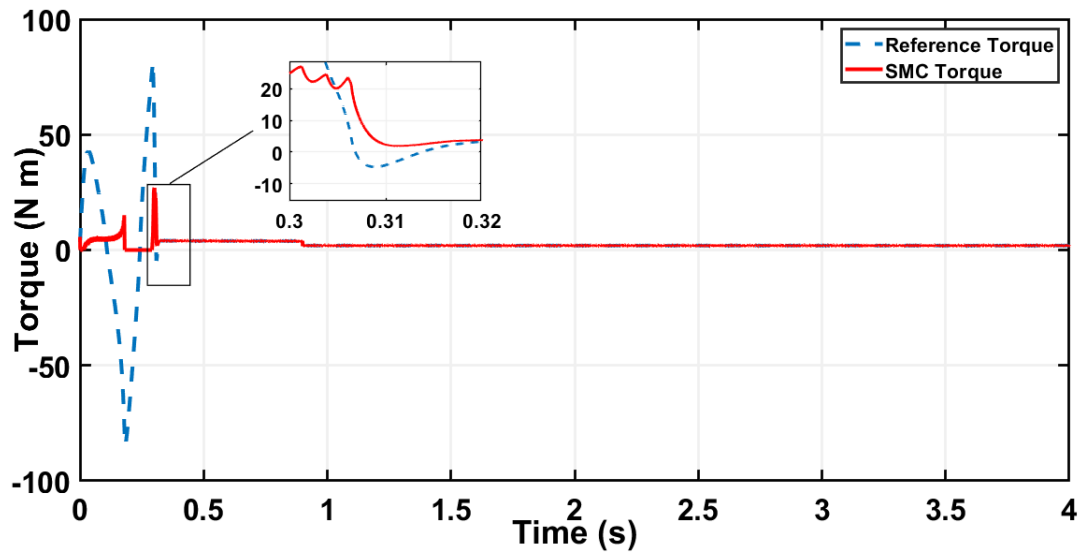
**Figure 5.11:** PI Result: Response of torque.



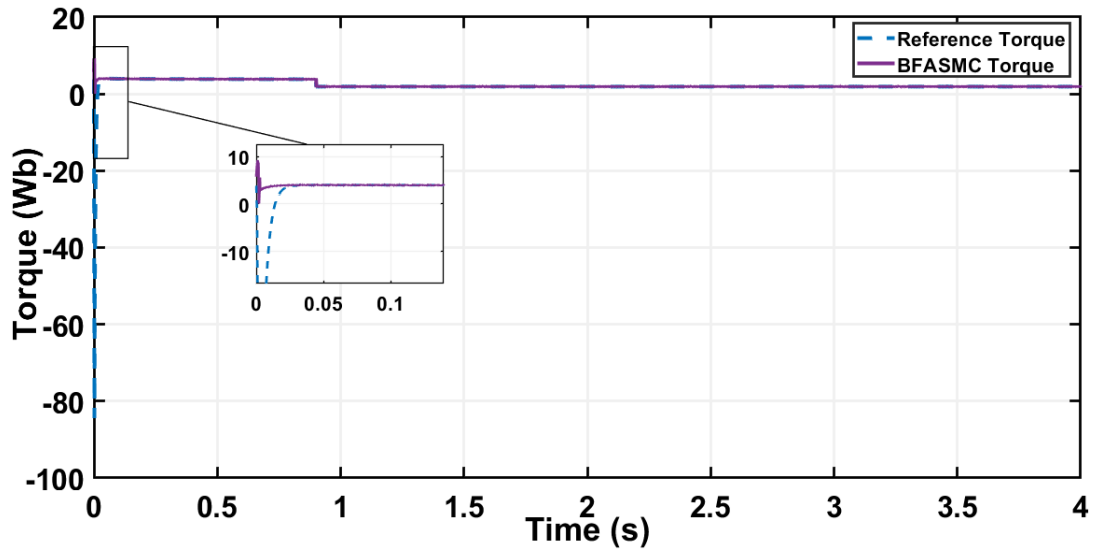**Figure 5.12:** SMC Result: Response of torque
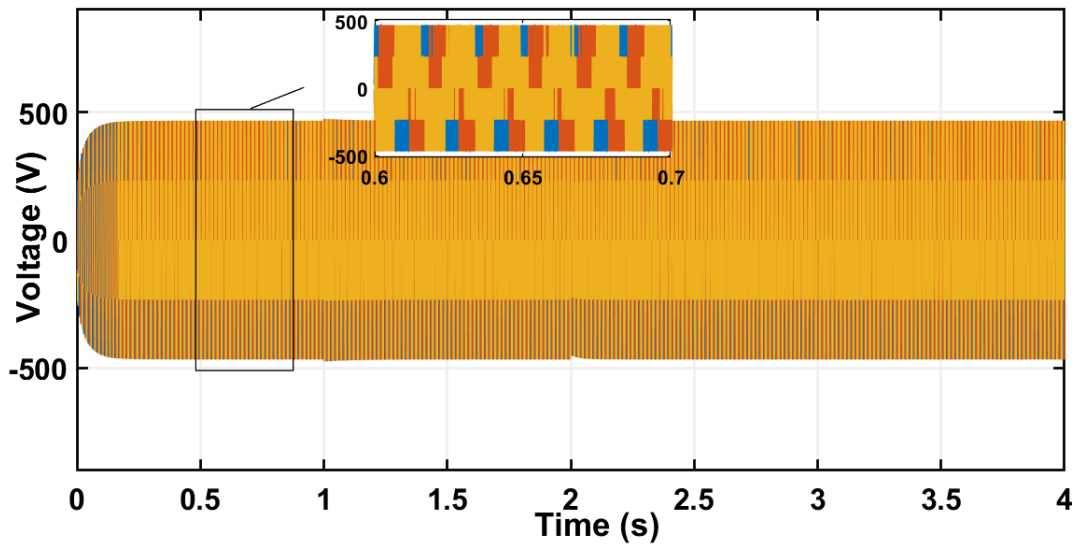
**Figure 5.13:** BFASMC Result: Response of torque.



**Figure 5.14:** Stepped output of three phase 3-level inverter.

**Table 5.2:** Parameters of power sources

| Sources | Specifications |
| --- | --- |
| Fuel cell | 350V, 250A, 34KW |
| Battery | 288V, 13.9Ah, Li-ion |
| Super-capacitor | 205V, 2700F |
| PV | 275V, 5A, 1.3KW |

**Table 5.3:** Parameters for SMC and BFASMC

| Parameter | Values |
| --- | --- |
| **SMC** | |
| $A_1, A_2, A_3, A_4, A5$ | $3000, 2000, 1500, 1500, 1000$ |
| $c_1, c_2, c_3, c_4, c_5$ | $5, 1, 1, 1, 1$ |
| $\alpha, \beta, \gamma, \zeta, \delta$ | $0.8, 0.5, 0.5, 0.7, 0.8$ |
| $\rho_1, \rho_2, \rho_3, \rho_4, \rho_5$ | $0.5, 0.5, 0.5, 0.5, 0.5$ |
| **BFASMC** | |
| $\overline{N}$ | $3000$ |
| $\phi_1, \phi_2, \phi_3, \phi_4, \phi_5$ | $10000, 10000, 20000, 30000, 10000$ |

dated in real-time by establishing the setup of real-time controller hardware in the loop . The controller of the C2000 Delfino MCU F28379D Launchpad is used to create discrete values for the plant model's control laws on MATLAB/Simulink. Furthermore, the findings obtained from this C-HIL arrangement are compared with those produced from MATLAB/Simulink simulations to validate the controller's response in the real-time analysis. In Fig.(5.15)-(5.17), it is shown that the controller operating in real-time produces some oscillations while tracking the reference values .The reason behind the oscillations is noise produced due to the conversion of control inputs from PWM to analog. Nonetheless, it can be concluded from this result that our proposed controller is performing efficiently while tracking the DC bus and speed value to reference value.
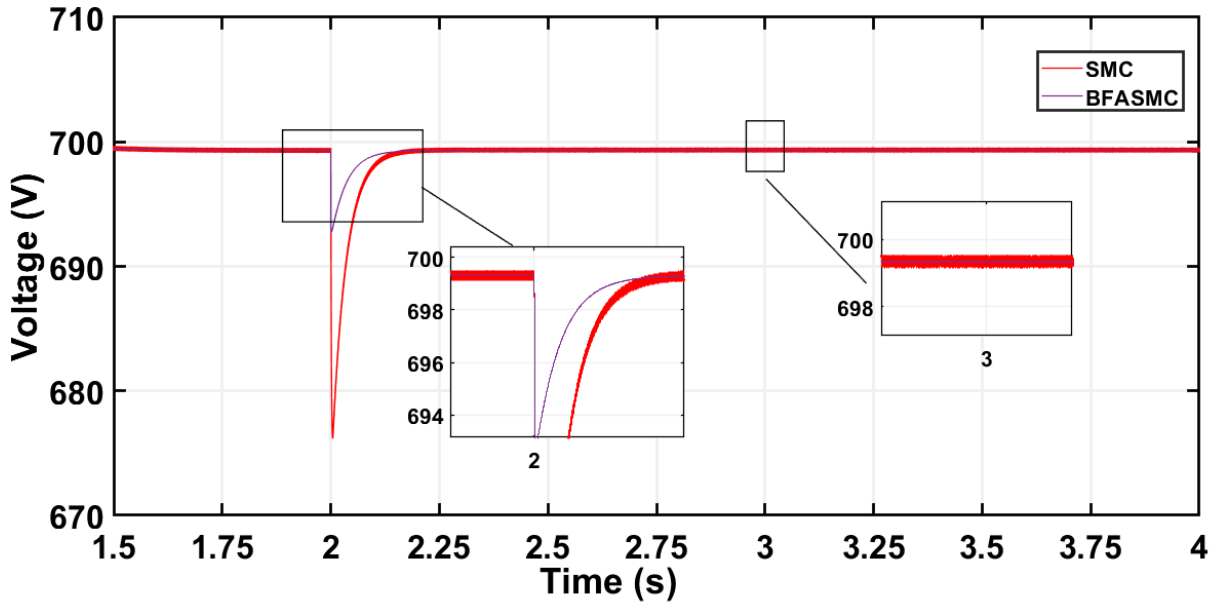
**Figure 5.15:** HIL response for DC bus voltage $v_{dc}$
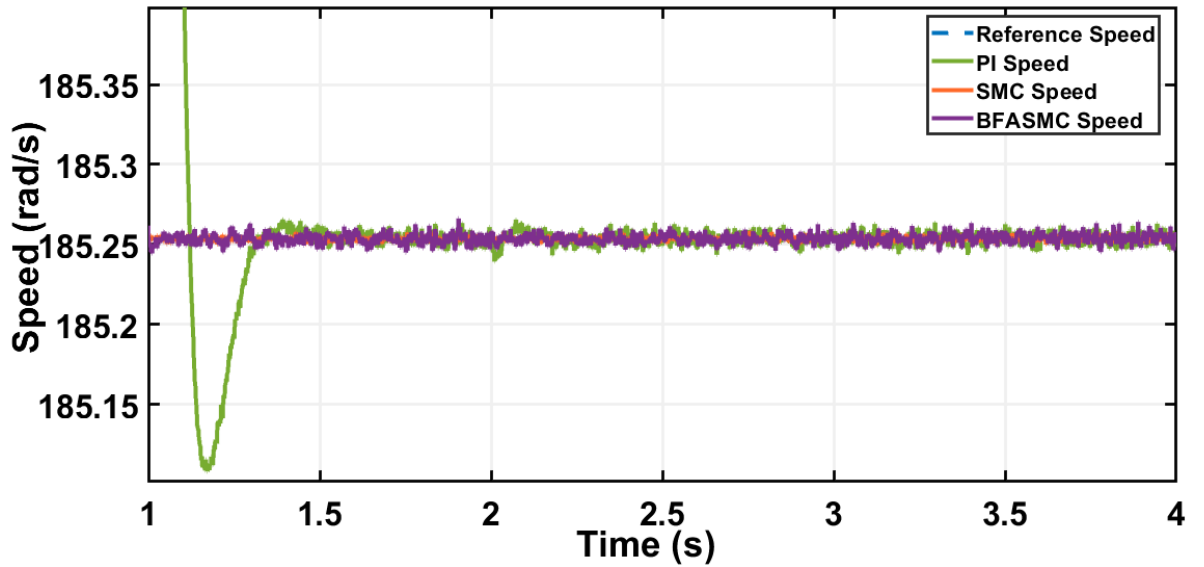


**Figure 5.16:** HIL response for speed

**Table 5.4:** Performance evaluation of proposed control schemes for DC Bus voltage regulation

| Control Strategy | ISE | IAE | ITAE |
|---|---|---|---|
| **SMC** | | | |
| $e_1$. | 5.119 | 0.1559 | 0.1317 |
| $e_2$. | 2.166 | 0.1347 | 0.2443 |
| $e_3$. | 0.6403 | 0.06613 | 0.12 |
| $e_4$. | 2.385 | 0.03115 | 0.04853 |
| **BFASMC** | | | |
| $e_1$. | 1.385 | 0.07273 | 0.08944 |
| $e_2$. | 0.1683 | 0.02004 | 0.02861 |
| $e_3$. | 0.03445 | 0.01324 | 0.02032 |
| $e_4$. | 0.01089 | 0.05615 | 0.09311 |

*Note:IAE integral absolute error, ISE integral square error,ITAE integral time absolute error*

**Table 5.5:** Performance evaluation of proposed control schemes for Induction motor model

| Control Strategy | ISE | IAE | ITAE |
|---|---|---|---|
| **PI** | | | |
| Speed | 4.243 | 1.176 | 0.6394 |
| Flux | 2.166 | 0.1347 | 0.2443 |
| Torqu | 0.0008646 | 0.02326 | 0.01513 |
| **SMC** | | | |
| Speed | 0.001994 | 0.008889 | 0.004256 |
| **BFASMC** | | | |
| Speed | 0.0008322 | 0.004214 | 0.002193 |

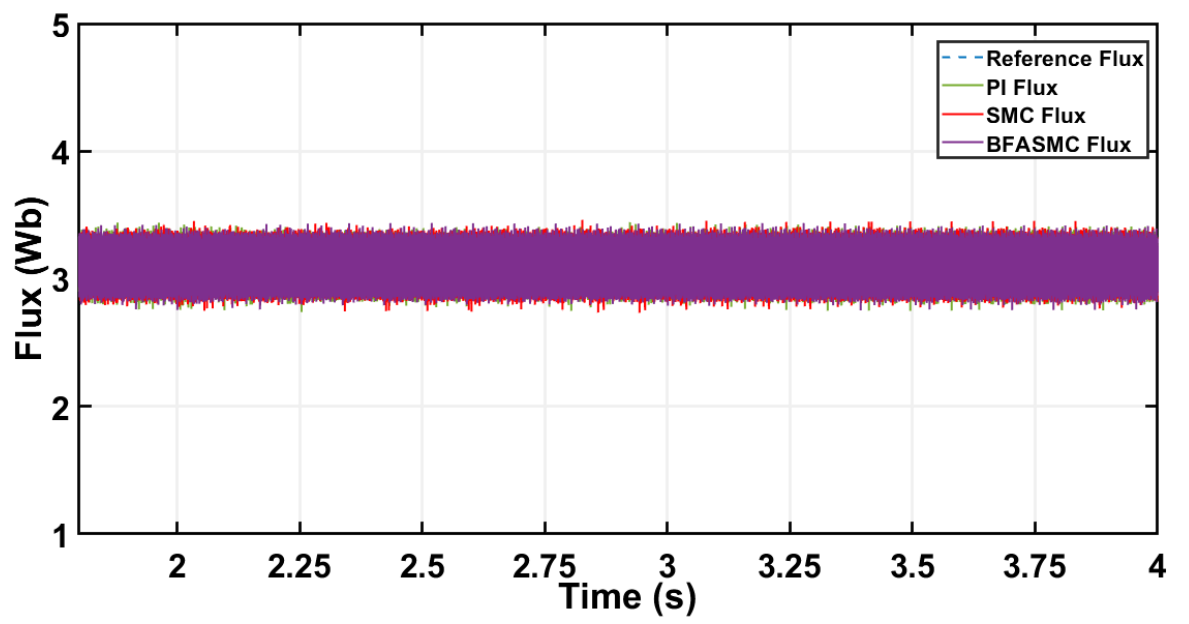*Note:IAE integral absolute error, ISE integral square error, ITAE integral time absolute error*

**Figure 5.17:** HIL response for flux

CHAPTER 6

# Conclusion

This research offers the BFASMC technique for DC bus voltage and speed tracking of EV.The HESS of EV comprised of FC, battery, SC, and PV. The performance of proposed controller has been evaluated using MATLAB/Simulink under varying load conditions and comparison has been made with SMC. The Lyapunov stability criteria is used to prove controller's stability. The results show that BFASMC outperforms the other tested controller. The primary goal of the proposed controller is to correctly stabilize and track the DC bus voltage and speed of motor to the target values. BFASMC does not require knowledge of upper bound of disturbance and its gain is not over-estimated which reduces chattering. The performance of BFASMC is robust and efficient, with no steady-state error. Finally, hardware-in-loop studies on C2000 Delfino platform validate the controller's feasibility using real-time analysis.[2]

## 6.1   Future Work

In future different converter topologies and diffrent controllers can be used for dc bus voltage and speed tracking of induction motor.The variations in speed of induction motor can be studied under different fault conditions.Different inverter topology can be utilized.Different energy sources can be used in HESS.One of the upcoming tasks can be hardware prototype.

# Bibliography

[1] Kamran Zeb et al. "Performance of adaptive PI based on fuzzy logic for Indirect Vector Control Induction Motor drive". In: *2016 2nd International Conference on Robotics and Artificial Intelligence (ICRAI)*. 2016, pp. 93–98. DOI: 10.1109/ICRAI.2016.7791235.

[2] Hussein Obeid et al. "Barrier function-based adaptive sliding mode control". In: *Automatica* 93 (2018), pp. 540–544. ISSN: 0005-1098. DOI: https://doi.org/10.1016/j.automatica.2018.03.078. URL: https://www.sciencedirect.com/science/article/pii/S0005109818301742.

[3] Kamran Zeb et al. "Robust speed regulation of indirect vector control induction motor using fuzzy logic controllers based on optimization algorithms". In: *Electrical Engineering* 100 (2018), pp. 787–802.

[4] Yanwei Liu et al. "Multi-objective optimization of energy management strategy on hybrid energy storage system based on radau pseudospectral method". In: *IEEE Access* 7 (2019), pp. 112483–112493.

[5] Zheng Chen et al. "Stochastic model predictive control for energy management of power-split plug-in hybrid electric vehicles based on reinforcement learning". In: *Energy* 211 (2020), p. 118931.

[6] Jie Hu et al. "Intelligent energy management strategy of hybrid energy storage system for electric vehicle based on driving pattern recognition". In: *Energy* 198 (2020), p. 117298.

[7] Renzong Lian et al. "Rule-interposing deep reinforcement learning based energy management strategy for power-split hybrid electric vehicle". In: *Energy* 197 (2020), p. 117297.

[8] Ana-Maria Petri and Dorin Petreus. "Vector Control of Induction Machine Used in Electric Vehicle". In: *2020 43rd International Spring Seminar on Electronics Technology (ISSE)*. IEEE. 2020, pp. 1–5.

[9] Aqeel Ur Rahman, Iftikhar Ahmad, and Ali Shafiq Malik. "Variable structure-based control of fuel cell-supercapacitor-battery based hybrid electric vehicle". In: *Journal of Energy Storage* 29 (2020), p. 101365.

[10] Syed Ahmad Siffat et al. "Robust integral backstepping control for unified model of hybrid electric vehicles". In: *IEEE Access* 8 (2020), pp. 49038–49052.

[11] Yitao Wu et al. "A predictive energy management strategy for multi-mode plug-in hybrid electric vehicles based on multi neural networks". In: *Energy* 208 (2020), p. 118366.

[12] Bo Yang et al. "Applications of battery/supercapacitor hybrid energy storage systems for electric vehicles using perturbation observer based robust control". In: *Journal of Power Sources* 448 (2020), p. 227444.

[13] Yang Zhou, Alexandre Ravey, and Marie-Cecile Péra. "Multi-mode predictive energy management for fuel cell hybrid electric vehicles using Markov driving pattern recognizer". In: *Applied Energy* 258 (2020), p. 114057. ISSN: 0306-2619. DOI: https://doi.org/10.1016/j.apenergy.2019.114057. URL: https://www.sciencedirect.com/science/article/pii/S0306261919317441.

[14] Pierpaolo Polverino, Ivan Arsie, and Cesare Pianese. "Optimal energy management for hybrid electric vehicles based on dynamic programming and receding horizon". In: *Energies* 14.12 (2021), p. 3502.

[15] Aqeel Ur Rahman et al. "Fuzzy supertwisting sliding mode-based energy management and control of hybrid energy storage system in electric vehicle considering fuel economy". In: *Journal of Energy Storage* 37 (2021), p. 102468.

[16] Tzu-Chia Chen et al. "Development of machine learning methods in hybrid energy storage systems in electric vehicles". In: *Mathematical Problems in Engineering* 2022 (2022), pp. 1–8.

[17] Usama Ilyas et al. "Energy Optimization of Hybrid Energy Storage System (HESS) for Hybrid Electric Vehicle (HEV)". In: *Engineering Proceedings* 12.1 (2022), p. 75.

[18] Yogeshwar Balasaheb Najgad et al. "Advancement of hybrid energy storage system with PWM technique for electric vehicles". In: *2022 6th International conference on intelligent computing and control systems (ICICCS)*. IEEE. 2022, pp. 238–242.

[19] Germán Andrés Ramos and Ramon Costa-Castelló. "Energy management strategies for hybrid energy storage systems based on filter control: Analysis and comparison". In: *Electronics* 11.10 (2022), p. 1631.

[20] Hossein Rezaei et al. "Energy management strategies of battery-ultracapacitor hybrid storage systems for electric vehicles: Review, challenges, and future trends". In: *Journal of Energy Storage* 53 (2022), p. 105045.

[21] Yongpeng Shen et al. "An energy management strategy based on fuzzy logic for hybrid energy storage system in electric vehicles". In: *IEEJ Transactions on Electrical and Electronic Engineering* 17.1 (2022), pp. 53–60.

[22] Chun Wang, Rui Liu, and Aihua Tang. "Energy management strategy of hybrid energy storage system for electric vehicles based on genetic algorithm optimization and temperature effect". In: *Journal of Energy Storage* 51 (2022), p. 104314.